



RESEARCH MEMORANDUM

TUFT STUDIES OF THE FLOW OVER A WING AT
FOUR ANGLES OF SWEEP

By

Gerald Hieser

Langley Memorial Aeronautical Laboratory
Langley Field, Va.

FILE COPY

To be returned to
the files of the National
Advisory Committee
for Aeronautics
Washington, D. C.

**NATIONAL ADVISORY COMMITTEE
FOR AERONAUTICS**

WASHINGTON

July 10, 1947

NATIONAL ADVISORY COMMITTEE FOR AERONAUTICS

RESEARCH MEMORANDUM

TUFT STUDIES OF THE FLOW OVER A WING AT
FOUR ANGLES OF SWEEP

By Gerald Hieser

SUMMARY

Tuft studies of the flow over a semispan wing at sweep angles of 0° , 30° , 45° , and -45° were conducted in the Langley 16-foot high-speed tunnel at Reynolds numbers ranging from 3,300,000 to 18,000,000. The tufts show the deviation of flow direction from that of the free stream due to the induced velocities imparted to the air flow normal to the wing leading edge. The tufts also indicate that a pronounced spanwise flow occurs in the boundary layer near the trailing edge because of the spanwise pressure gradient which exists over a wing swept back or swept forward.

Studies of the stalling characteristics show that the stall begins at the tip and moves inboard with increasing angle of attack at positive sweep; the stall begins at root and moves outboard at negative sweep (sweepforward). At $\pm 45^\circ$ sweep the stall was less sharply defined than at the lower angles of sweep.

No effect of Mach number on the flow patterns as indicated by tufts was found in the speed range of these tests which extended to a Mach number of 0.55.

INTRODUCTION

It is shown in reference 1 that the flow pattern about a swept wing differs from that of an unswept wing. For the swept wing the component of velocity normal to the leading edge (the effective velocity) is changed in magnitude by the induced velocities, while the component parallel to the leading edge remains unchanged. The resulting difference in flow pattern about a swept wing causes changes in the load distribution and is thereby accompanied by changes in the force and moment characteristics.

The purpose of the present investigation is to present a tuft study of three-dimensional flow over a wing at various angles of

sweep. The results are given in the form of photographs of tufts on the upper surface of the wing and by sketches of streamlines interpreted from the tuft patterns. The data are presented for sweep angles of 0° , 30° , 45° , and -45° (sweepforward), over an angle-of-attack range, and for tunnel speeds ranging from $M = 0.13$ to $M = 0.55$. The corresponding range of Reynolds number based on mean chord measured parallel to the air stream was from about 3.3 million to 18 million. A comparison of the low-speed stalling characteristics of the wing at the various sweep angles is shown by the tuft photographs and sketches showing the streamlines. In addition, calculated streamlines over the wing at a representative angle of attack for the different sweep angles are presented for comparison with the flow indicated by tufts. The data presented herein are one phase of a general investigation of the effects of sweep on the aerodynamic characteristics of the present wing.

SYMBOLS

M	free-stream Mach number
Λ	angle of sweep measured from the direction normal to the tunnel longitudinal axis, degrees
α	geometric angle of attack, degrees
x/c	ratio of distance along the chord to the chord length measured from the leading edge

APPARATUS AND METHODS

A 10-foot semispan NACA 65₂-215 wing which had a mean chord of 3.333 feet and tapered linearly from a root chord of 4.44 feet to 2.222 feet at the tip in the unswept configuration was used for the present study in the Langley 16-foot high-speed tunnel. The wing had no dihedral or twist and the airfoil sections were normal to the 1/4-chord line and parallel to the tunnel longitudinal axis at 0° sweep. The wing was mounted with the root at the tunnel wall and was pivoted at the 50-percent chord station of the root to obtain sweep. A different wing tip for each sweep angle was used so that the tip was parallel to the tunnel longitudinal axis. The over-all dimensions of the wing are given in table I for each sweep configuration. The model is shown mounted in the tunnel at sweep angles of 0° , 30° , and 45° in figure 1.

Wool tufts, 2 inches long, were arranged in rows on the upper surface of the wing at various spanwise stations parallel to the tunnel air stream. In order to compare the direction of flow over the wing as indicated by tufts with the free-stream direction, strips of black masking tape were located on the surface at various spanwise stations parallel to the tunnel longitudinal axis. With one exception, the tufts located between the closely spaced strips of tape (see figs. showing tuft photographs) were mounted on wire masts at different heights above the surface, varying from surface level near the leading edge to $1\frac{1}{4}$ inches near the trailing edge.

The elevated tufts were located so that they would be out of the boundary layer at small angles of attack. With the wing at 0° sweep the tufts between the closely spaced strips of tape nearest the root and tip were all mounted on the wing surface. The remaining tufts were also on the wing surface and were held in position by Scotch cellulose tape.

Since there was considerable leakage of air between the tunnel test section and the test chamber, leakage deflector plates were installed to reduce the effect of air leakage on the flow about the wing surface. Figure 2 shows the details of the plates which were located $1/2$ inch from the tunnel wall and extended 2 inches from the upper and lower surfaces of the wing.

In order to ascertain whether or not the thick boundary layer of the tunnel wall affected the flow about the wing with sweep, a $1/8$ -inch steel plate was installed parallel to the tunnel axis 5 inches from the tunnel wall. (The thickness of the boundary layer at the test section has been determined as 5 inches.) The plate extended 18 inches above and below the wing surface and curved smoothly to points 6 inches ahead of the leading edge and behind the trailing edge.

RESULTS AND DISCUSSION

Tuft photographs were obtained at the same test conditions both with and without the tunnel boundary-layer plate installed on the wing at a sweep of 45° . The pictures (fig. 3) were obtained at a Mach number of 0.13 and at angles of attack of 10° and 14° . As can be seen, no significant change in the flow characteristics, with and without the plate, is indicated by the tufts. Hence, all ensuing photographs were attained without the plate installed.

The tuft patterns over the wing at each sweep angle for a geometric angle of attack of 6° and a Mach number of 0.55 are shown

in figure 4. A sketch of the wing at each configuration of figure 4 showing the streamlines is presented in figure 5. The solid lines on the sketches represent streamlines indicated by surface tufts and the dashed lines show streamlines indicated by rows of elevated tufts. With the wing unswept (figs. 4(a) and 5) the tufts show that the direction of flow over the surface was parallel to the free stream except at the rear portion of the tip and in the boundary layer along the trailing edge where the flow was inward. The inflow resulted from the spanwise pressure gradient which is present on all finite span wings. The tufts indicate that the flow outside the boundary layer at the trailing edge remained parallel to the free stream. In the boundary layer the component of inflow is large relative to the velocity in the free-stream direction; however, above the boundary layer the inflow is small in relation to the free-stream component. Hence, the effect of inflow is noted only by the tufts in the boundary layer. The deviation of flow from the free-stream direction which existed beyond the 50-percent chord station near the wing root was due to the wake of the small pivot pin bracket. This influence extended over only a small portion of the wing surface. At sweep angles of 30° and 45° (figs. 4 and 5), the air experienced an inward flow over the forward portion of the wing. This flow was caused by the increase in the velocity component normal to the leading edge. As the air progressed further across the surface, the decrease in the induced velocity of the normal component resolved the resultant flow in a direction parallel to the free stream. In the boundary layer near the trailing edge a spanwise flow toward the tip existed which resulted from the pronounced spanwise pressure gradient (normal to the free stream) due to sweep. As in the case of the unswept wing, the spanwise flow is large as compared to the boundary-layer flow in the free-stream direction, but is small in relation to the stream vector above the boundary layer. Hence, the outward flow is shown by the surface tufts but does not affect the elevated tufts. In the case of $\Lambda = -45^\circ$ (sweepforward) shown in figures 4(b) and 5, the spanwise flow over the front portion of the wing, due to changes imparted to the effective velocity, was outward. The spanwise flow near the trailing edge, which is inward at sweepforward, was more pronounced than the outward flow for the 45° swept-back configuration. The inward flow at sweepforward was indicated by both the surface tufts and the elevated tufts.

Tuft photographs of the wing at the various sweep angles for a geometric angle of attack of 6° and a Mach number of 0.2 are presented in figure 6. A comparison of the tufts in this figure with those in figure 4 shows that no effect of Mach number on the flow pattern existed in the range from $M = 0.2$ to $M = 0.55$.

Figure 7 presents calculated streamlines over the wing at each sweep angle for a geometric angle of attack of 6° . The calculations were based on pressure distributions measured at the spanwise station 52 inches from the root ($52 \cos \Lambda$). The distributions were measured when no tufts were on the wing and were cross-faired so that the pressures were determined along chord lines parallel to the free stream. The direction of the flow at any chordwise station was calculated assuming that the induced velocity corresponding to the pressure coefficient was imparted to the velocity vector normal to the leading edge. The resultants of the components normal to the leading edge and parallel to the leading edge were determined and the tangents of the angles between the free-stream direction and the resultant components were plotted against corresponding chordwise stations. The streamlines were then derived by integration of the resulting curve from the leading edge to various chordwise stations.

A similarity of the patterns of streamlines outside the boundary layer shown in figures 4 and 5 and the calculated patterns of figure 7 can be noted. The spanwise flow in the boundary layer near the trailing edge due to the spanwise pressure gradients were not included in the calculations of figure 7.

Figure 8 shows the tuft patterns over the wing at an angle of attack of 0° , Mach number of 0.55, and sweep angles of 0° , 30° , 45° , and -45° . Due to low induced velocities and small spanwise pressure gradients, the flow was, in general, parallel to the free stream at all sweep angles.

The tuft patterns over the wing at geometric angles of attack from 8° through the stalling angles at a Mach number of 0.13 for sweep angles of 0° , 30° , 45° , and -45° are presented in figures 9, 11, 13, and 15, respectively. These figures are supplemented by sketches of the wing showing streamlines interpreted from the tuft photographs. The sketches are presented in figures 10, 12, 14, and 16, and the streamlines are shown for several angles of attack at each sweep angle. They also include shaded areas where the flow is unsteady and thereby aid in showing the progress of stall over the wing.

Tuft surveys on the wing with no sweep (figs. 9 and 10) show that separation began at about 14° near the trailing edge and progressed toward the leading edge as the angle was increased. The stall progressed forward more rapidly near the center of the wing than at the root and tip. No tuft photographs were obtained beyond 20° angle of attack, however, force data indicated that a sharp stall occurred at 22° .

The patterns for 30° of sweep are presented in figures 11 and 12. In general, the progress of stall appeared similar to that of the 0° sweep configuration except that separation near the tip occurred earlier, and the spanwise flow along the rear portion of the wing was outward and more prominent. The tufts show a rapid transition of flow between 19° and 20° , denoting an abrupt stall.

The tuft surveys for the 45° sweep configuration are shown in figures 13 and 14 for angles of attack through the stalling range. These figures show that the flow patterns were similar to those for 30° of sweep except that separation at the tip began at a lower angle of attack for the 45° sweep configuration. A rapid change in the flow characteristics over the outer portion of the wing between 18° and 19° is indicated, denoting that an abrupt stall occurred at the tip only. Above 19° the progress of separation was gradual and moved from the tip and trailing edge to the inboard and forward portions of the wing. No abrupt stall over the wing in general is indicated at angles of attack up to 28° .

The tuft photographs for the -45° sweep configuration at angles of attack ranging from 8° to 28° are presented in figure 15. Sketches showing the patterns of streamlines are shown in figure 16. Some of the photographs at high angles of attack (fig. 15) were repeated since the entire wing could not be photographed without shifting the camera. Separation at -45° sweep began on the inboard portion of the wing at about 12° angle of attack and progressed outward slowly until an angle of 28° was reached where the wing was almost entirely stalled. An inward flow over the rear portion of the wing is shown clearly.

CONCLUDING REMARKS

Tuft studies of the flow over a semispan wing at sweep angles of 0° , 30° , 45° , and -45° show that a pronounced spanwise flow occurs in the boundary layer along the trailing edge at sweepback and sweepforward. This flow is outward at sweepback and inward at sweepforward.

The tufts show that stalling occurs more rapidly near the tip at positive angles of sweep than at 0° or negative sweep. At -45° sweep stalling begins at the root and moves outward as the angle of attack is increased. No abrupt stall over the wing in general occurred at 45° or -45° sweep.

No effect of Mach number on the flow pattern over a swept wing was indicated up to a Mach number of 0.55.

Langley Memorial Aeronautical Laboratory
National Advisory Committee for Aeronautics
Langley Field, Va.

REFERENCE

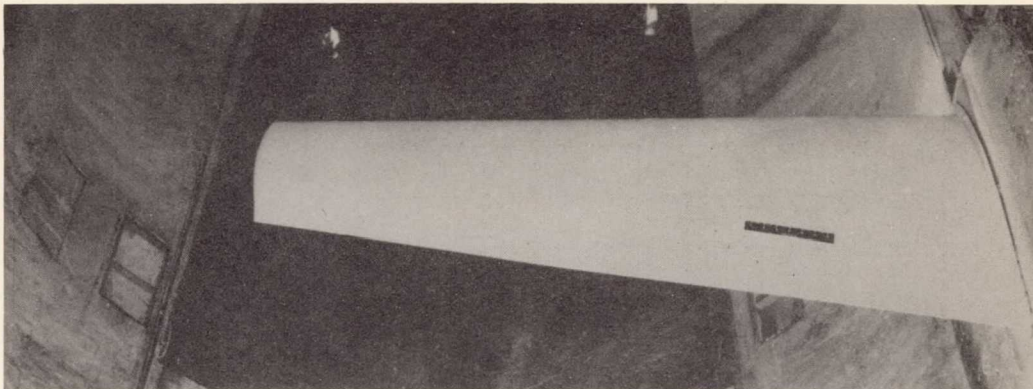
1. Jones, Robert T.: Wing Plan Forms for High-Speed Flight.
NACA TN No. 1033, 1946.

TABLE I

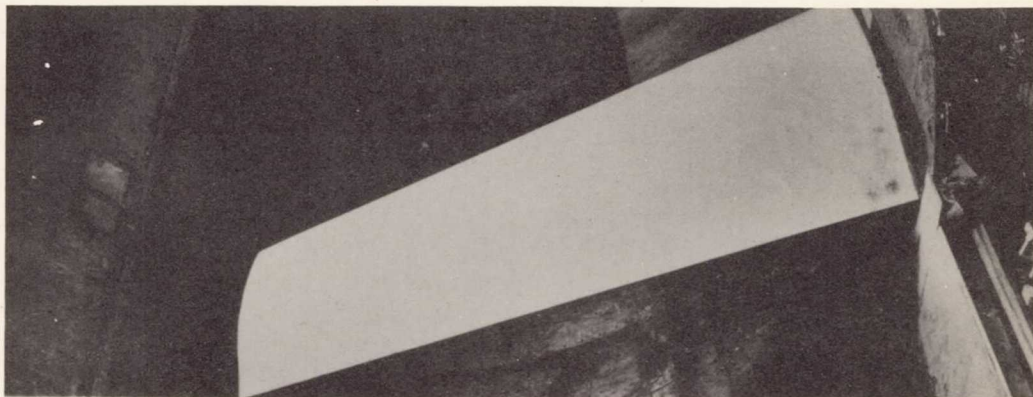
OVER-ALL DIMENSIONS OF WING

Sweep angle (Λ)	Root chord (ft)	Tip chord (ft)	Semispan (ft)
0	4.444	2.222	10
30	4.991	2.491	8.956
45	6.021	2.994	7.506
-45	6.750	3.350	6.721

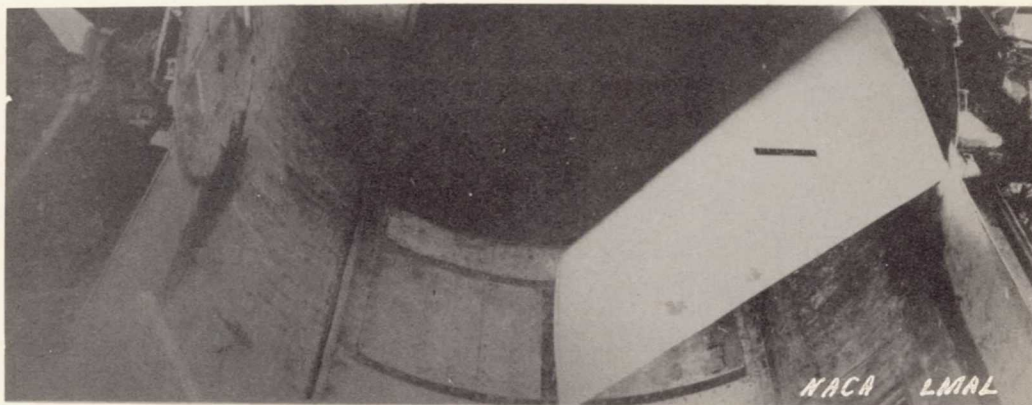
NATIONAL ADVISORY
COMMITTEE FOR AERONAUTICS



(a) $\Lambda = 0^\circ$.

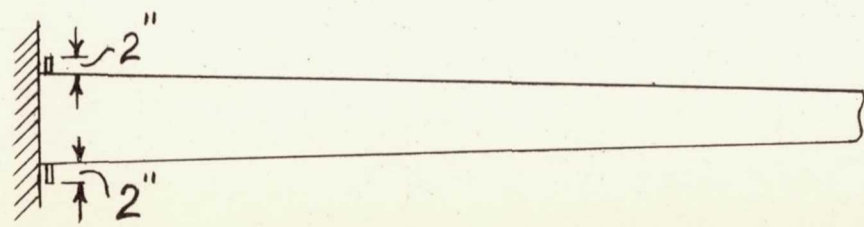
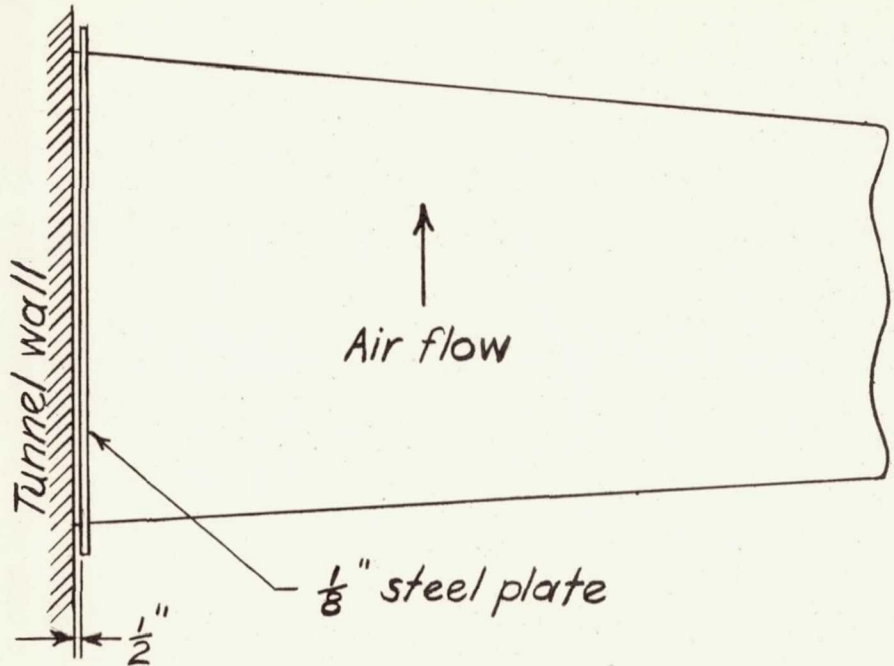


(b) $\Lambda = 30^\circ$.



(c) $\Lambda = 45^\circ$.

Figure 1.- 65_2 -215 wing mounted in 16-foot tunnel.



NATIONAL ADVISORY
COMMITTEE FOR AERONAUTICS

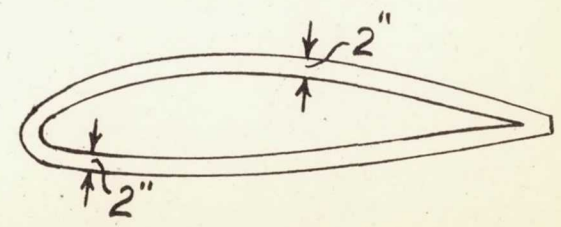
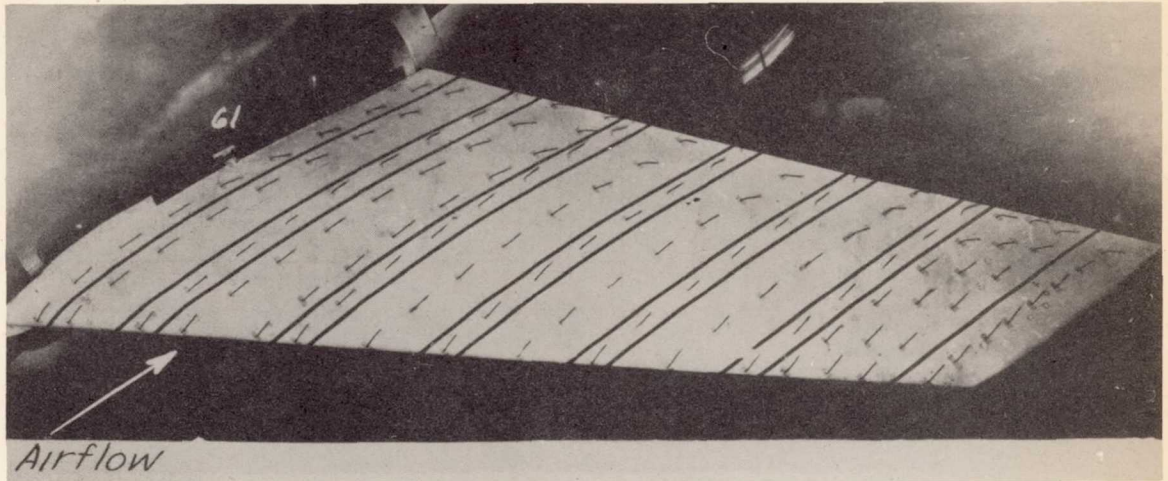
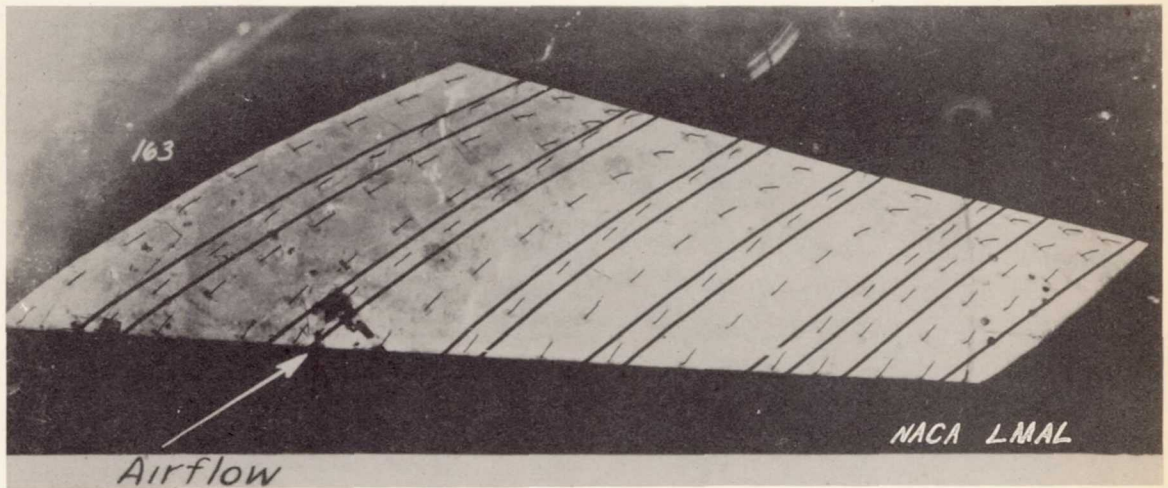


Figure 2.- Sketch showing location of leakage deflector plates.



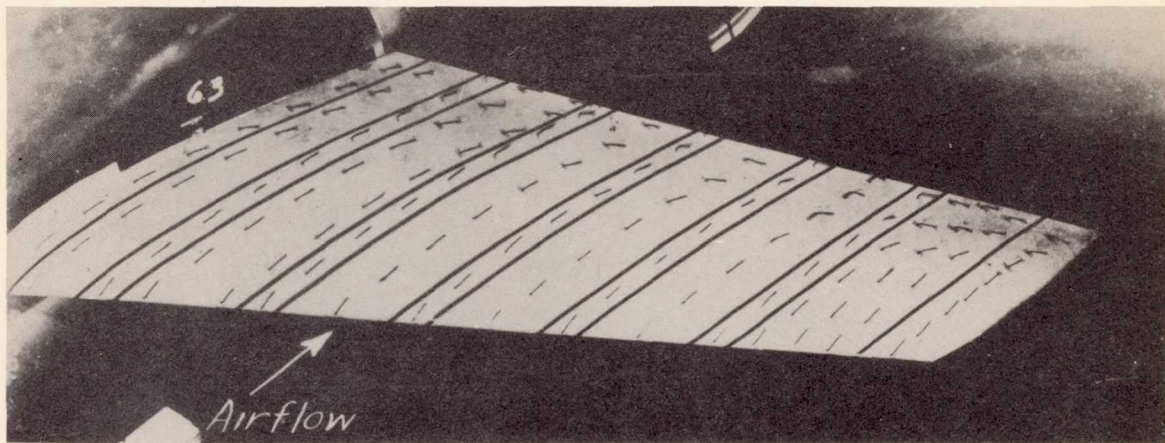
Boundary-layer plate not installed.



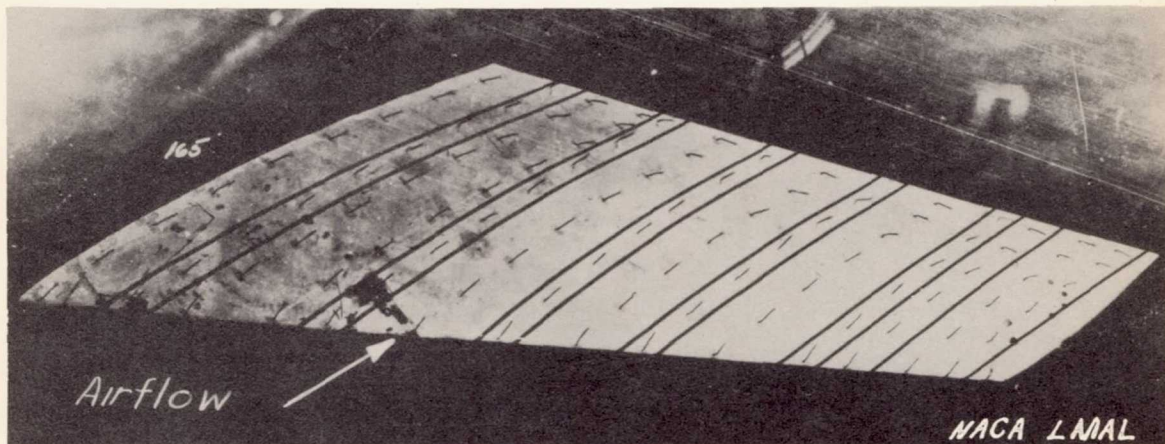
Boundary-layer plate installed.

(a) $\alpha = 10^\circ$.

Figure 3.- Tuft patterns on a 65_2 -215 wing with and without boundary-layer plate installed, $\Lambda = 45^\circ$, $M = 0.13$.



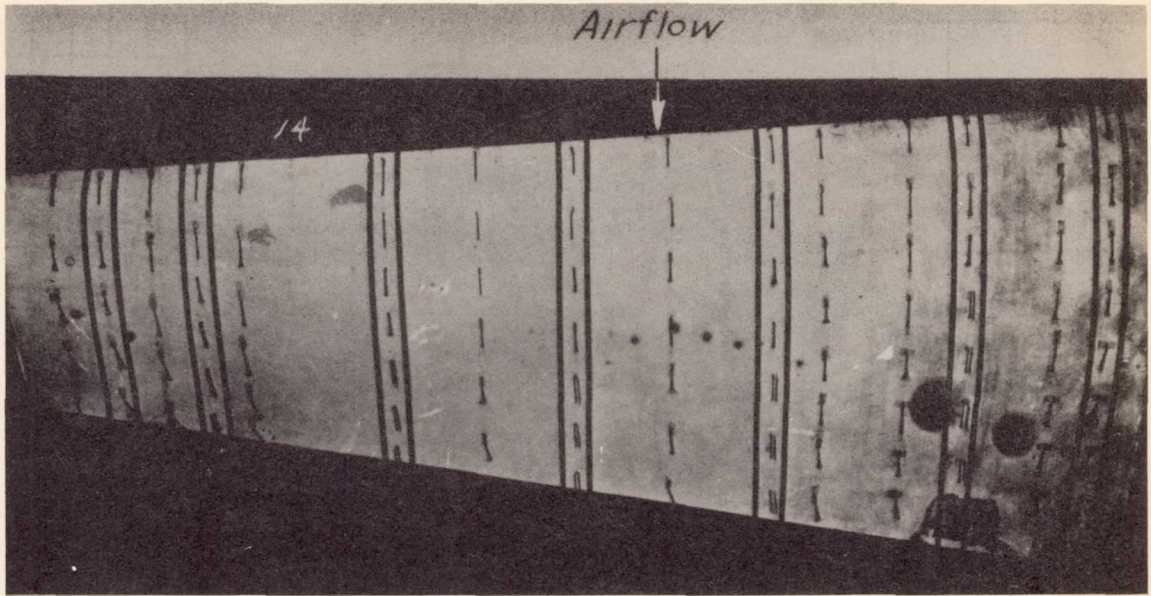
Boundary-layer plate not installed.



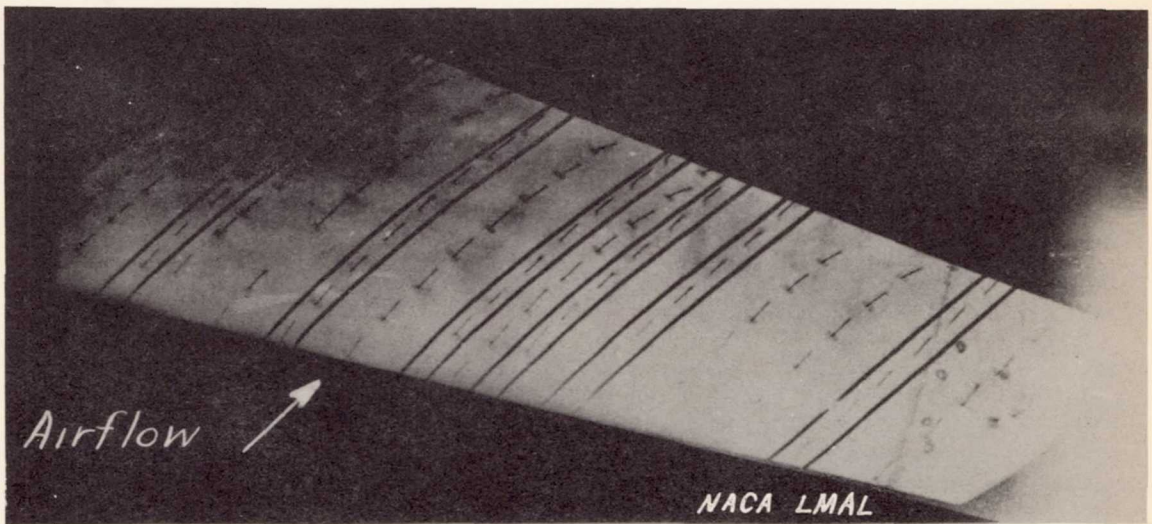
Boundary-layer plate installed.

(b) $\alpha = 14^\circ$.

Figure 3.- Concluded.



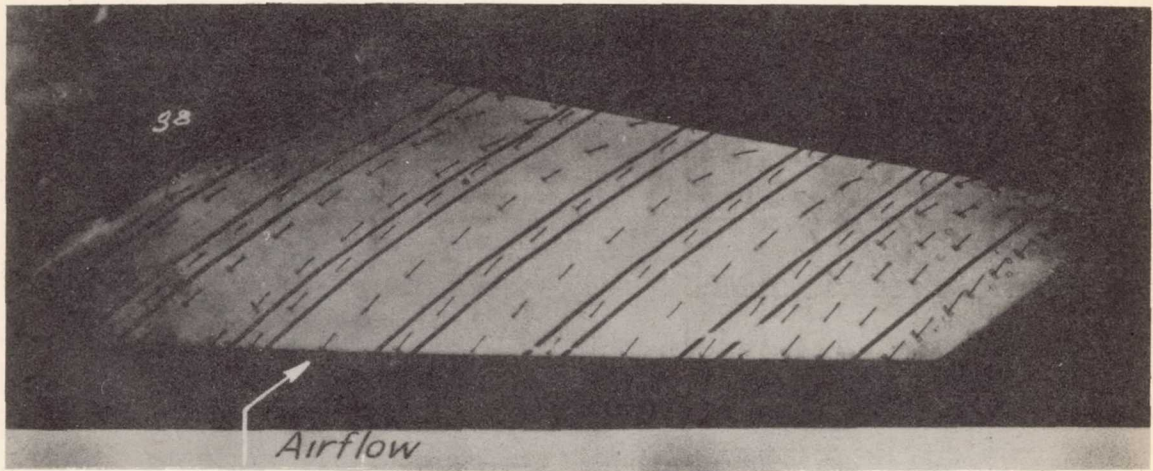
$$\Lambda = 0^\circ$$



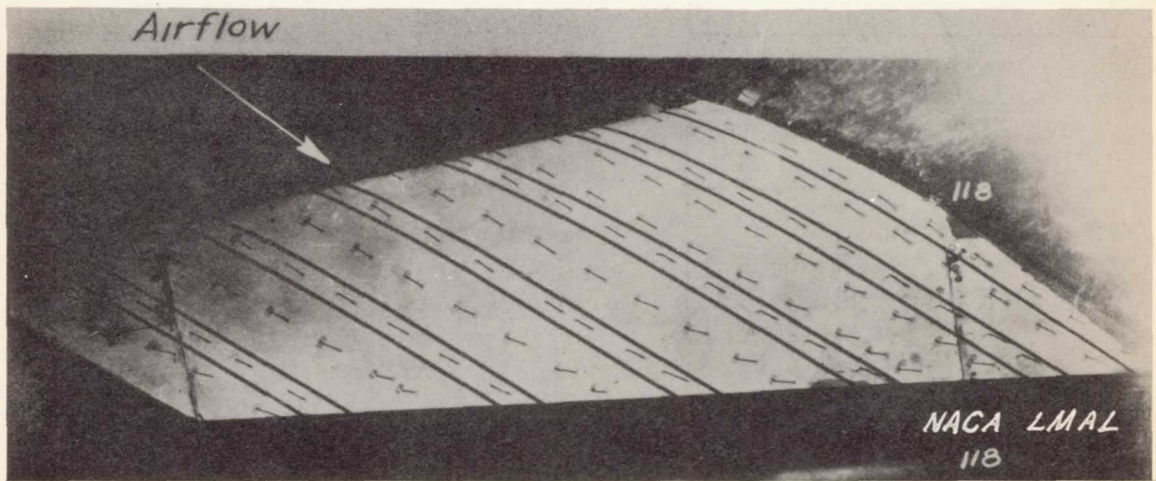
$$\Lambda = 30^\circ$$

(a) $\Lambda = 0^\circ, 30^\circ$.

Figure 4.- Tuft pattern on 65₂-215 wing, $\alpha = 6^\circ$, $M = 0.55$.



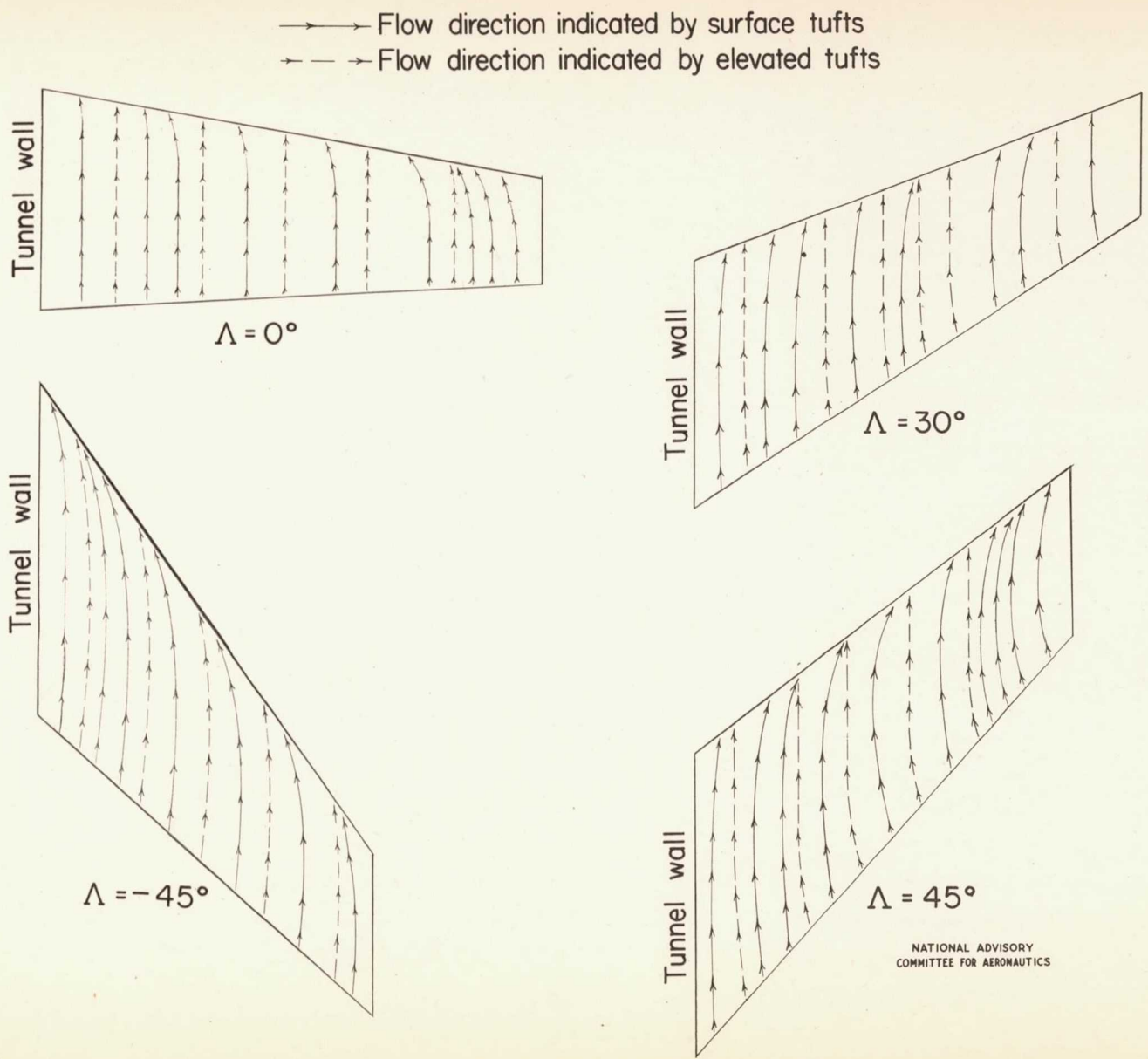
$$\Lambda = 45^\circ$$



$$\Lambda = -45^\circ$$

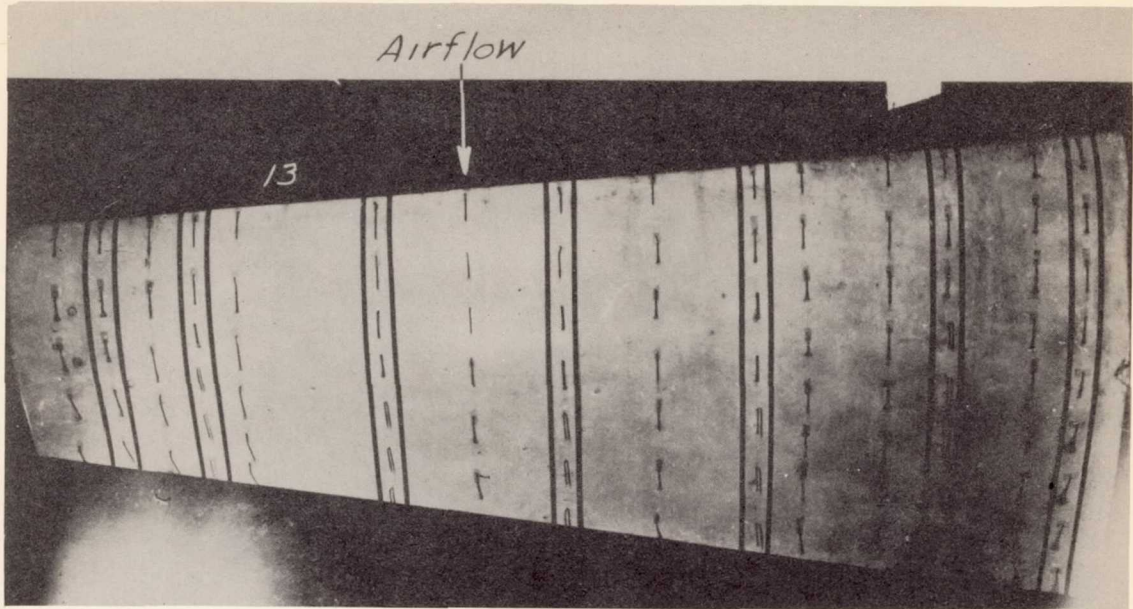
(b) $\Lambda = 45^\circ, -45^\circ$.

Figure 4.- Concluded.

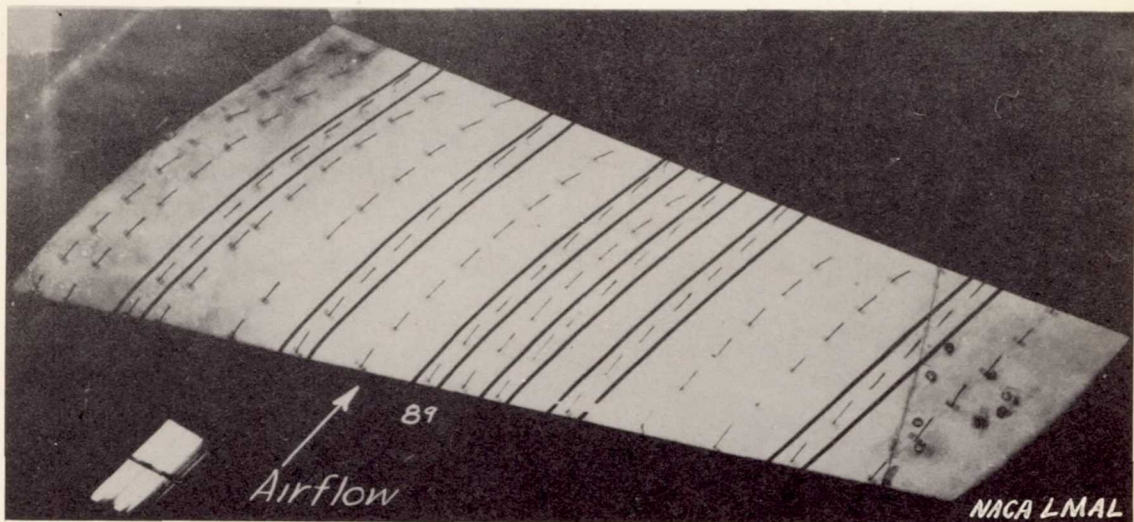


NATIONAL ADVISORY
COMMITTEE FOR AERONAUTICS

Figure 5.—Flow pattern indicated by tufts on a 65₂-215 wing at four sweep angles. $\alpha = 6^\circ$, $M = .55$.



$$\nu = 0^\circ$$



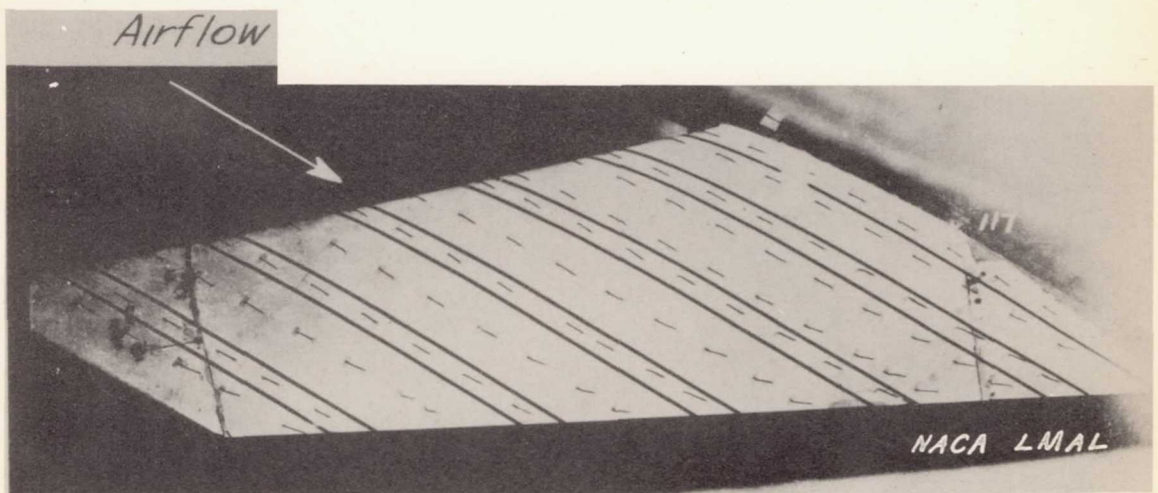
$$\Lambda = 30^\circ$$

(a) $\Lambda = 0^\circ, 30^\circ$.

Figure 6.- Tuft patterns on a 65₂-215 wing, $\alpha = 6^\circ$, $M = 0.2$.



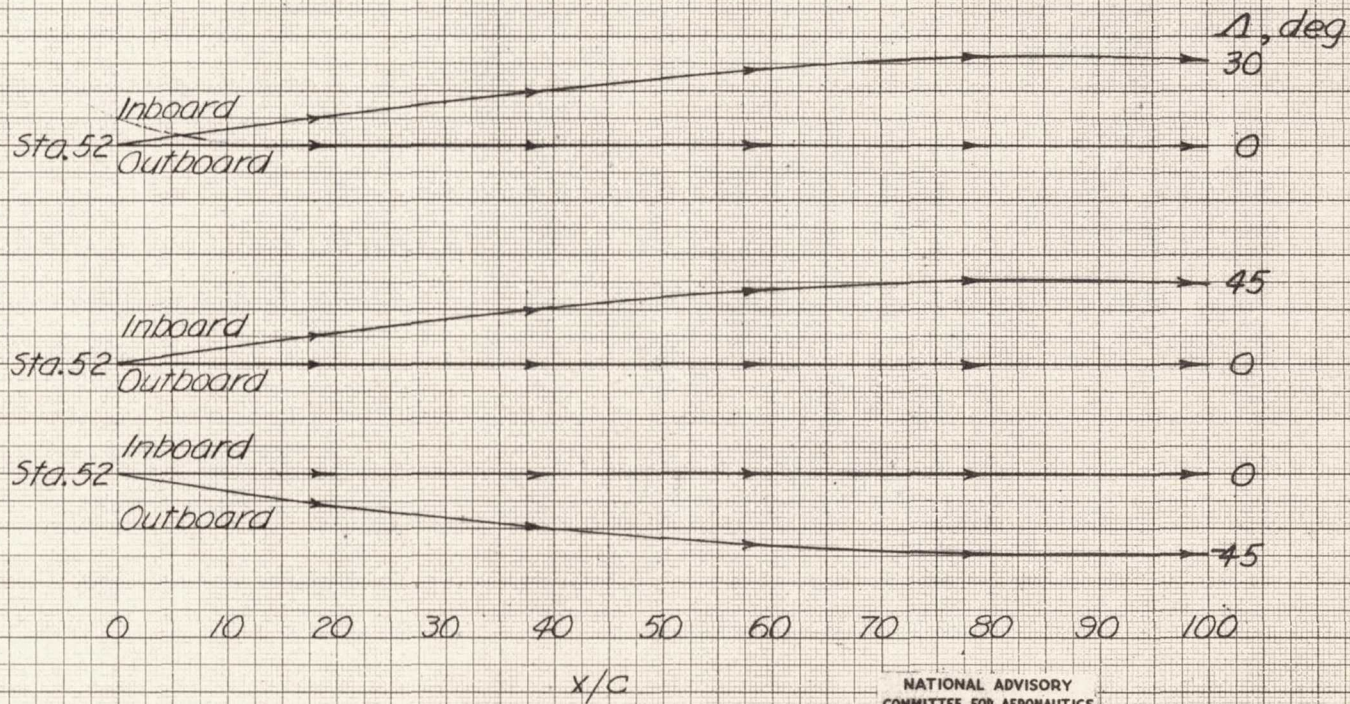
$$\Lambda = 45^{\circ}$$



$$\Lambda = -45^{\circ}$$

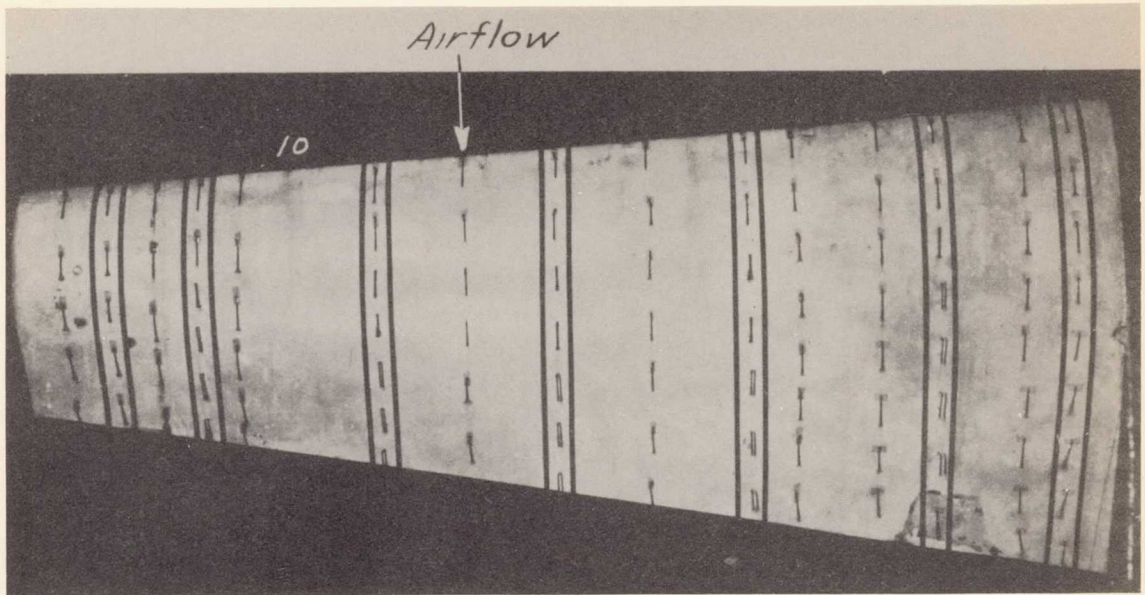
(b) $\Lambda = 45^{\circ}, -45^{\circ}$.

Figure 6.- Concluded.

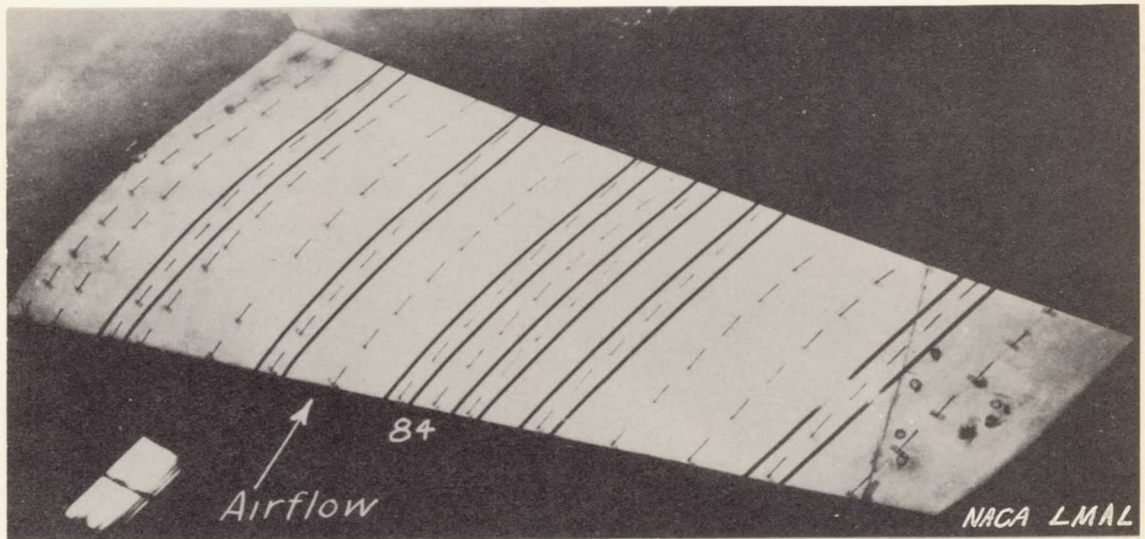


NATIONAL ADVISORY
COMMITTEE FOR AERONAUTICS

Figure 7.- Calculated streamlines over 65₂-215 wing at spanwise station 52 for the various sweep angles. $\alpha = 6^\circ$



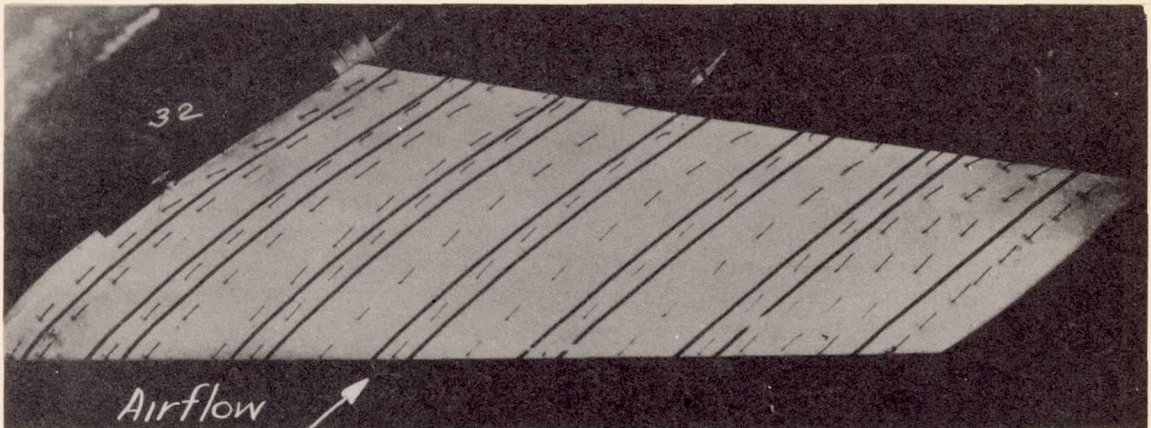
$$\Lambda = 0^\circ$$



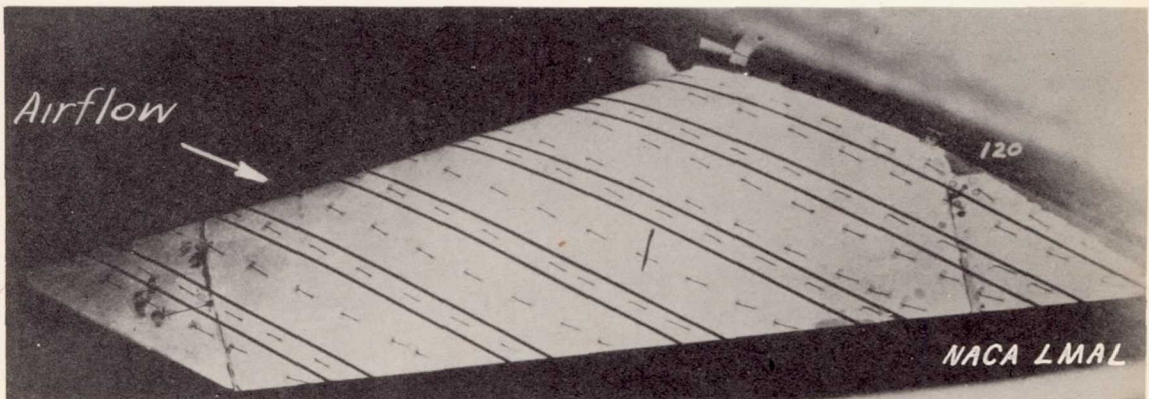
$$\Lambda = 30^\circ$$

(a) $\Lambda = 0^\circ, 30^\circ$.

Figure 8.- Tuft patterns on a 65₂-215 wing, $\alpha = 0^\circ$, $M = 0.55$.



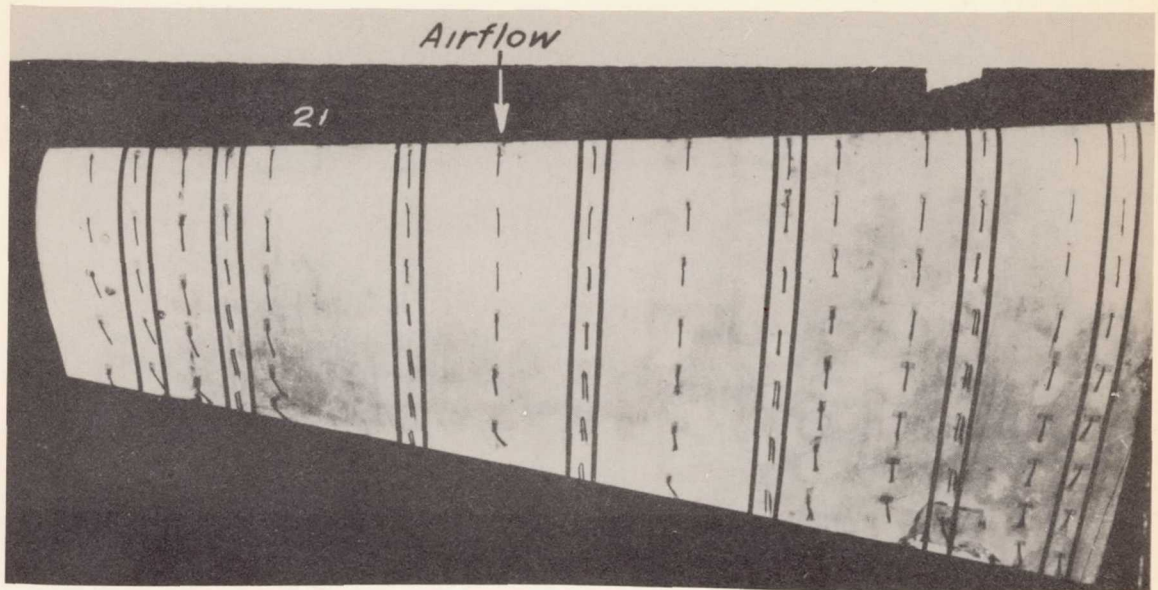
$$\Lambda = 45^\circ$$



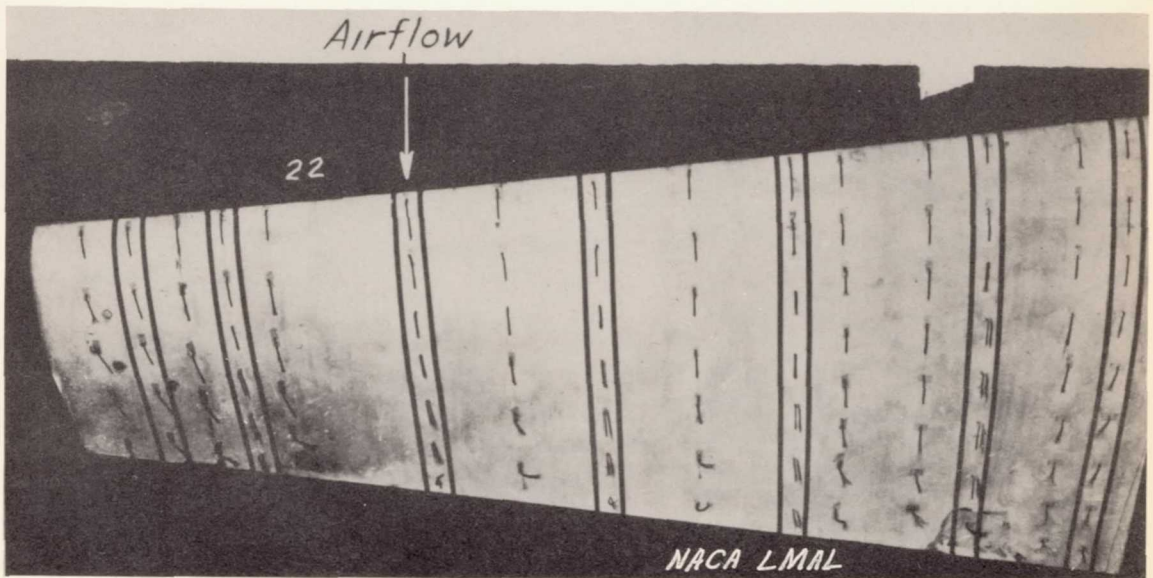
$$\Lambda = -45^\circ$$

(b) $\Lambda = 45^\circ, -45^\circ$.

Figure 8.- Concluded.



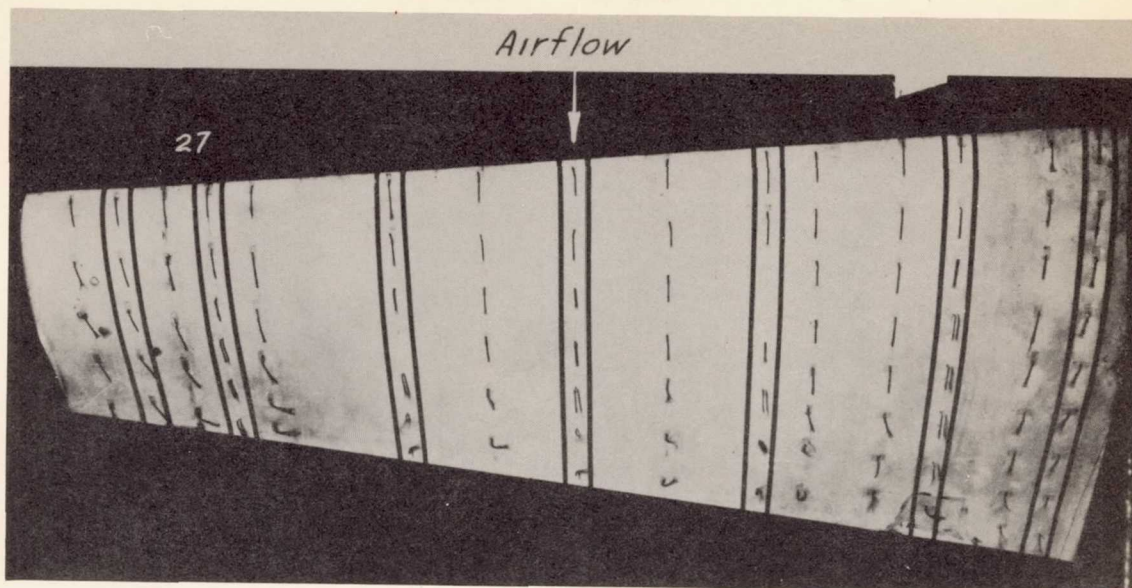
$\alpha = 10^\circ$



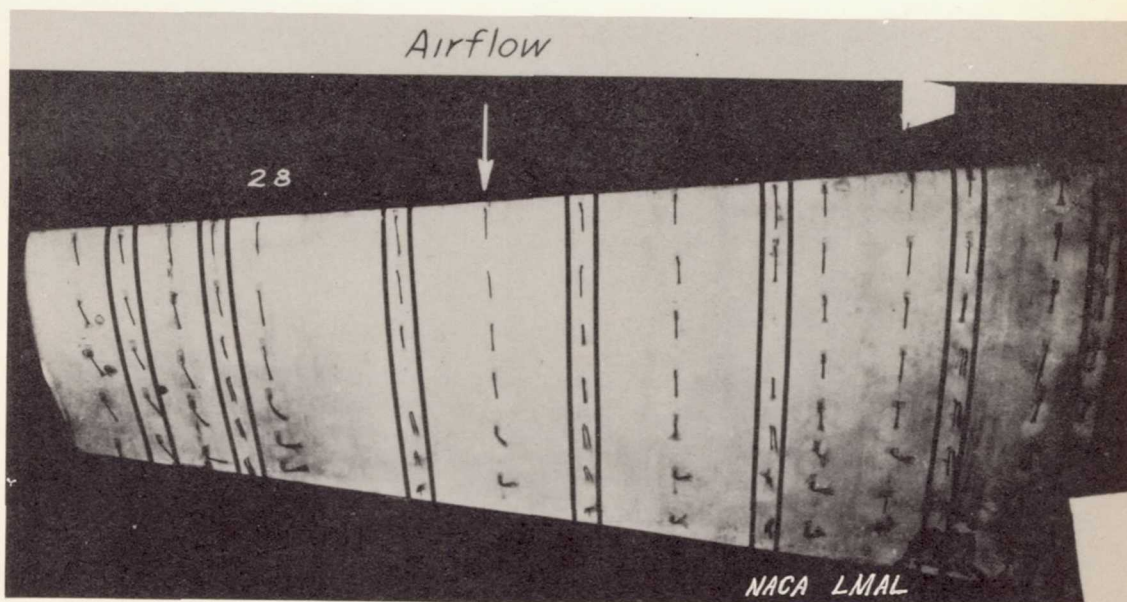
$\alpha = 14^\circ$

(a) $\alpha = 10^\circ, 14^\circ$.

Figure 9.- Tuft patterns on a 65₂-215 wing, $\Lambda = 0^\circ$, $M = 0.13$.



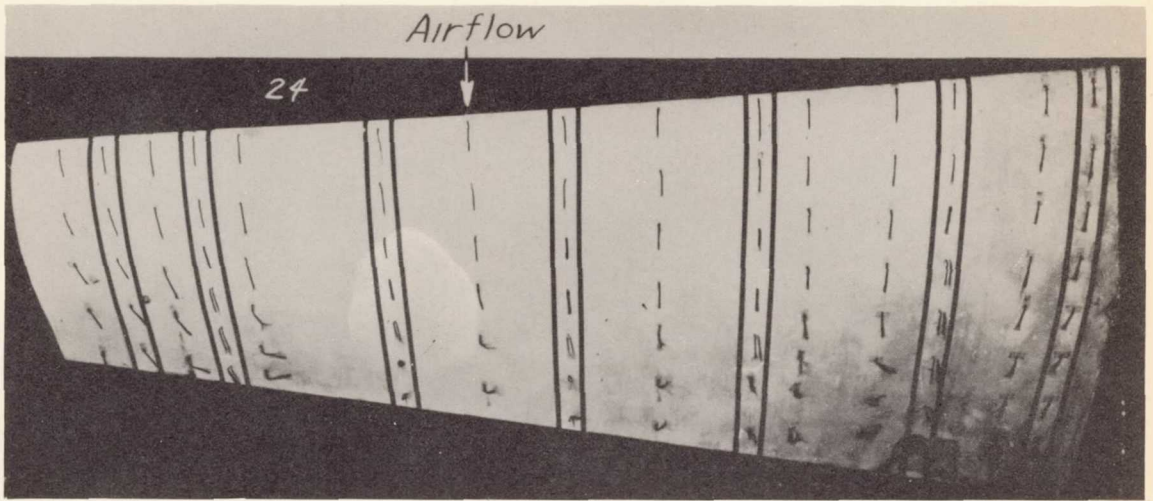
$$\alpha = 16^{\circ}$$



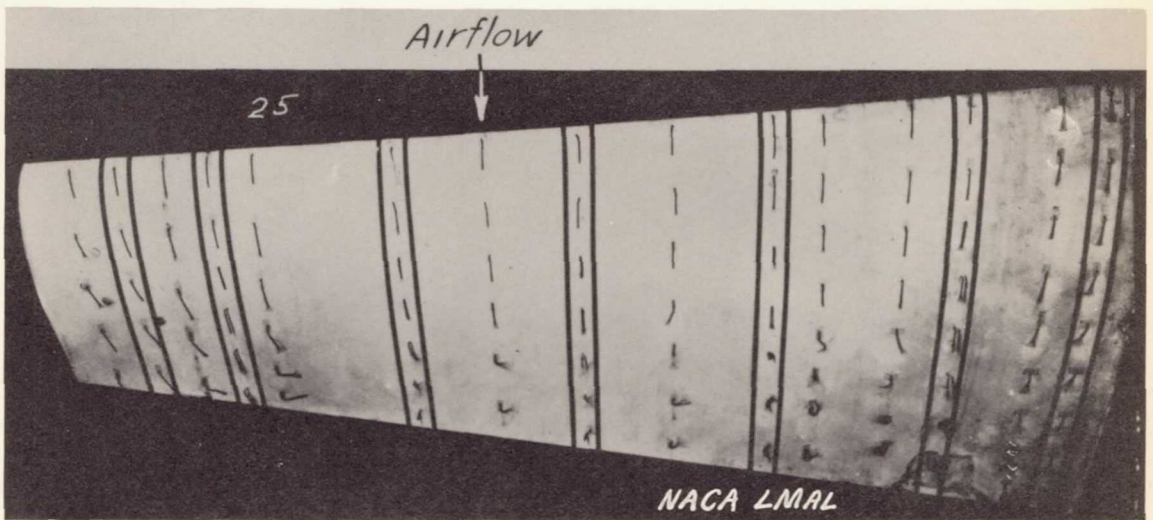
$$\alpha = 17^{\circ}$$

(b) $\alpha = 16^{\circ}, 17^{\circ}$.

Figure 9.- Continued.



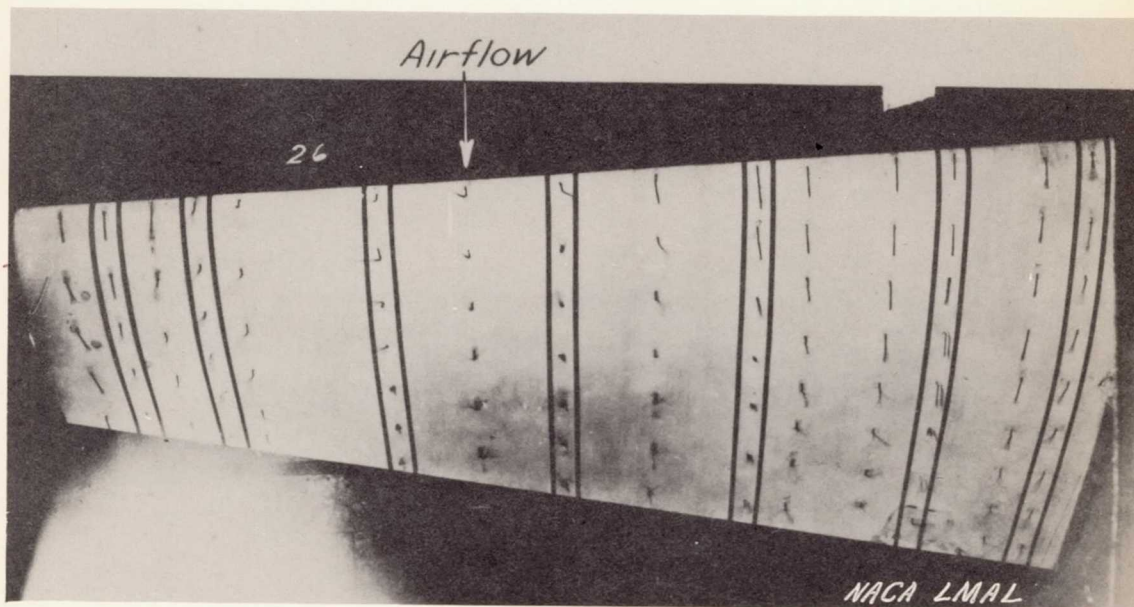
$\alpha = 18^\circ$



$\alpha = 19^\circ$

(c) $\alpha = 18^\circ, 19^\circ$.

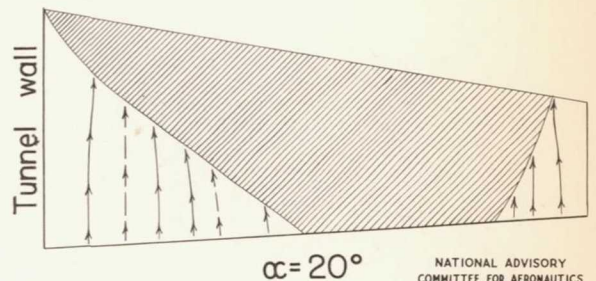
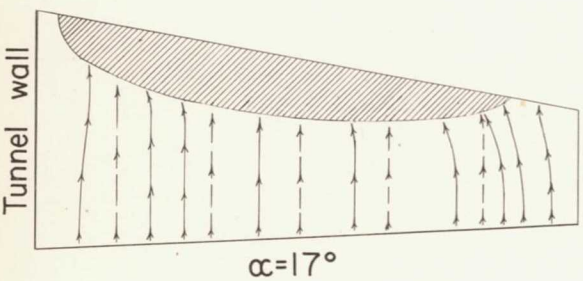
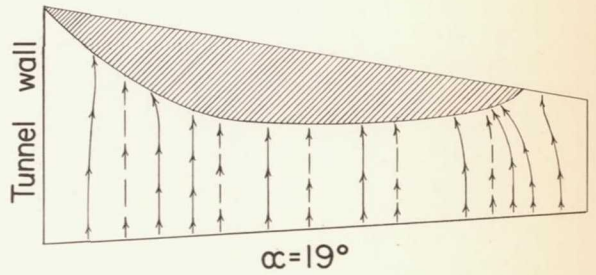
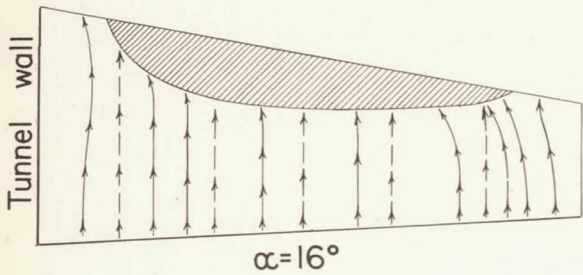
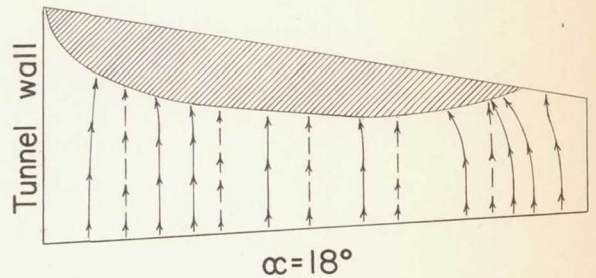
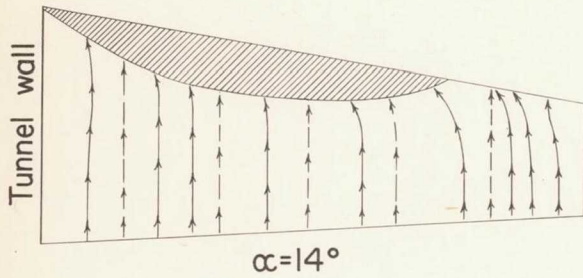
Figure 9.- Continued.



(d) $\alpha = 20^\circ$.

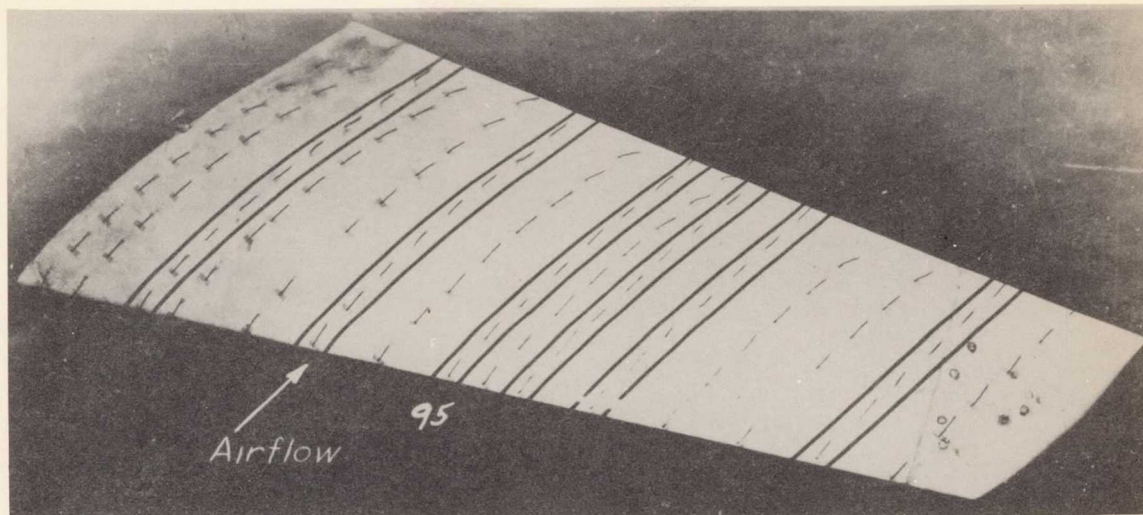
Figure 9.- Concluded.

- Flow direction indicated by surface tufts
- - - - Flow direction indicated by elevated tufts
- ▨ Region of unsteady flow

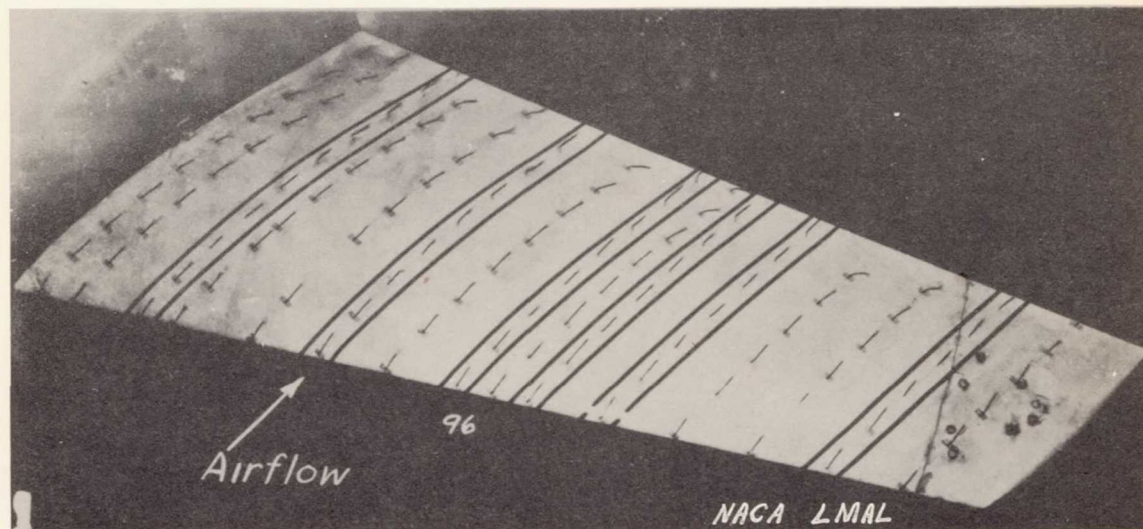


NATIONAL ADVISORY
COMMITTEE FOR AERONAUTICS

Figure 10.—Flow patterns indicated by tufts on a 65₂-215 wing at various angles of attack. $\Lambda = 0^\circ$. $M = .13$.



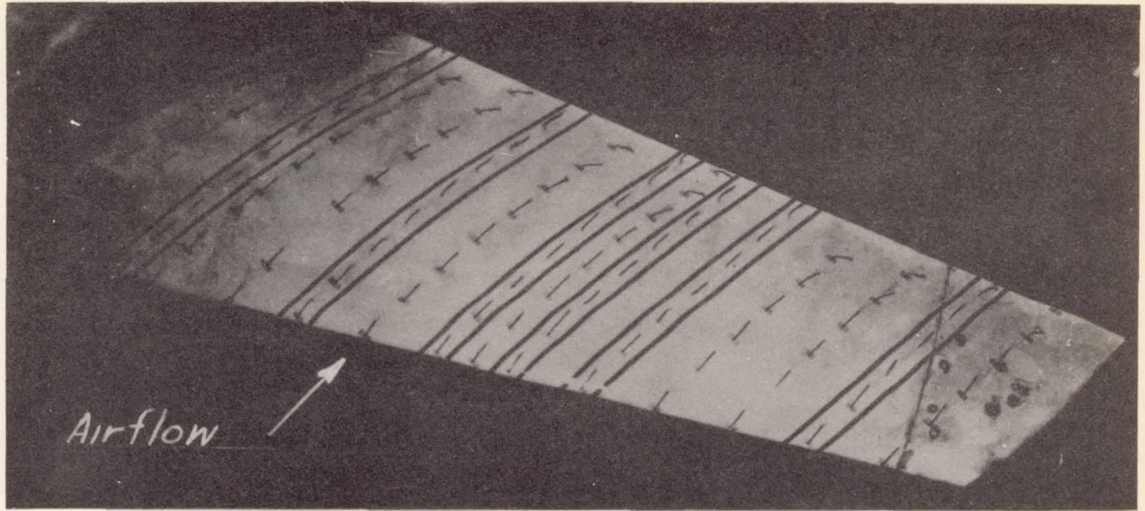
$$\alpha = 8^\circ$$



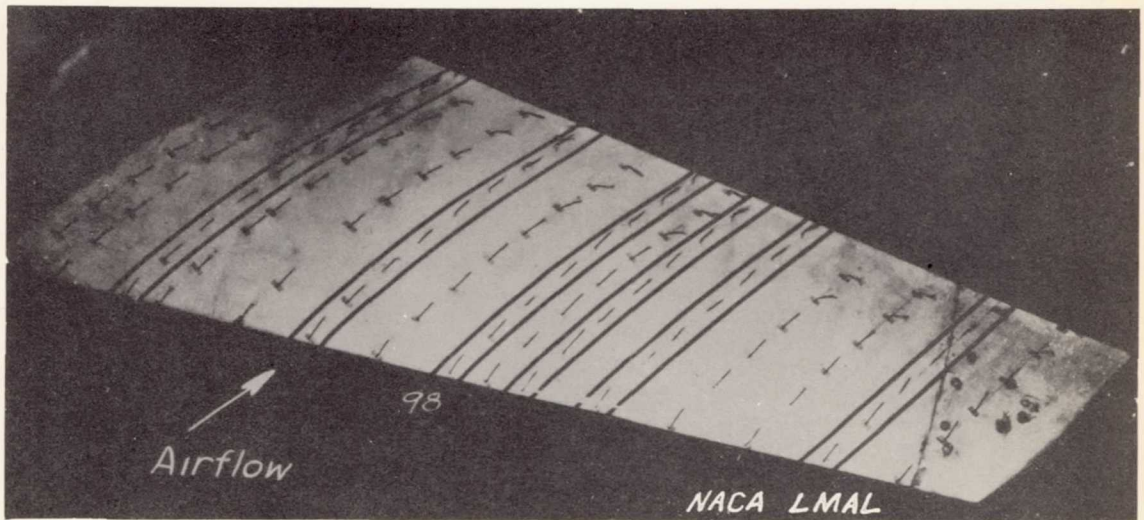
$$\alpha = 10^\circ$$

(a) $\alpha = 8^\circ, 10^\circ$.

Figure 11.- Tuft patterns on a 65_2 -215 wing, $\Lambda = 30^\circ$, $M = 0.13$.



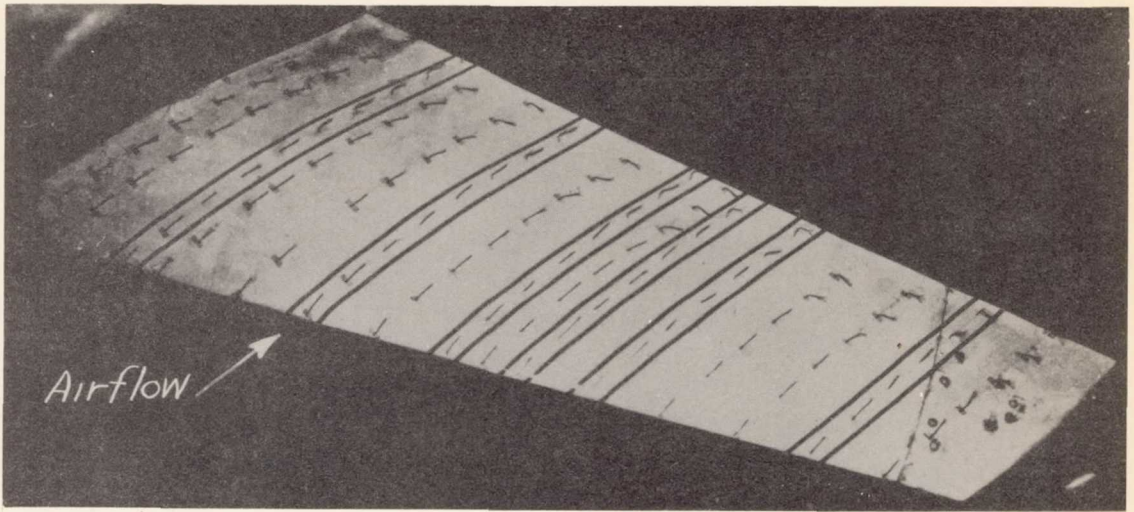
$$\alpha = 12^{\circ}$$



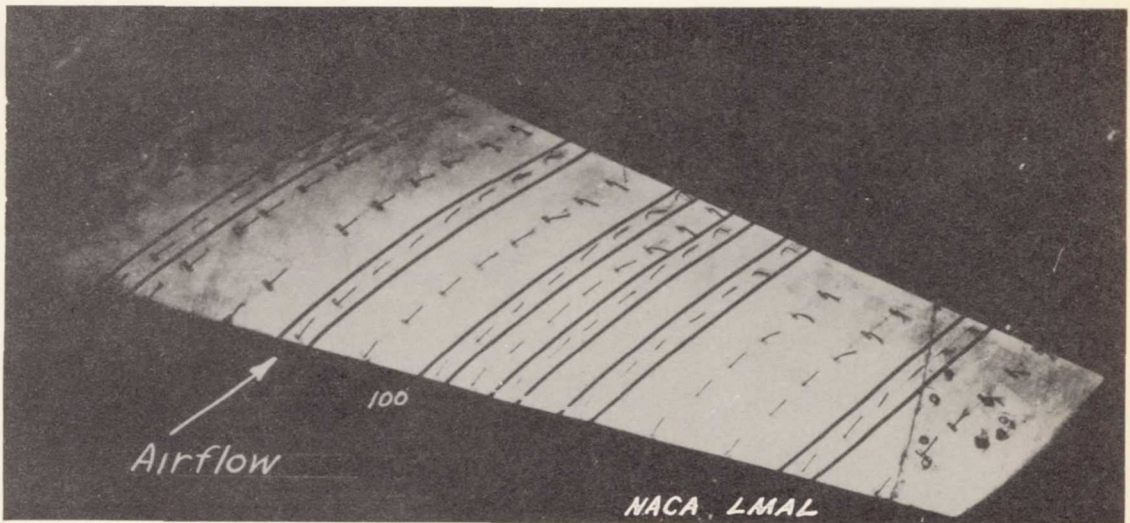
$$\alpha = 14^{\circ}$$

(b) $\alpha = 12^{\circ}, 14^{\circ}$.

Figure 11.- Continued.



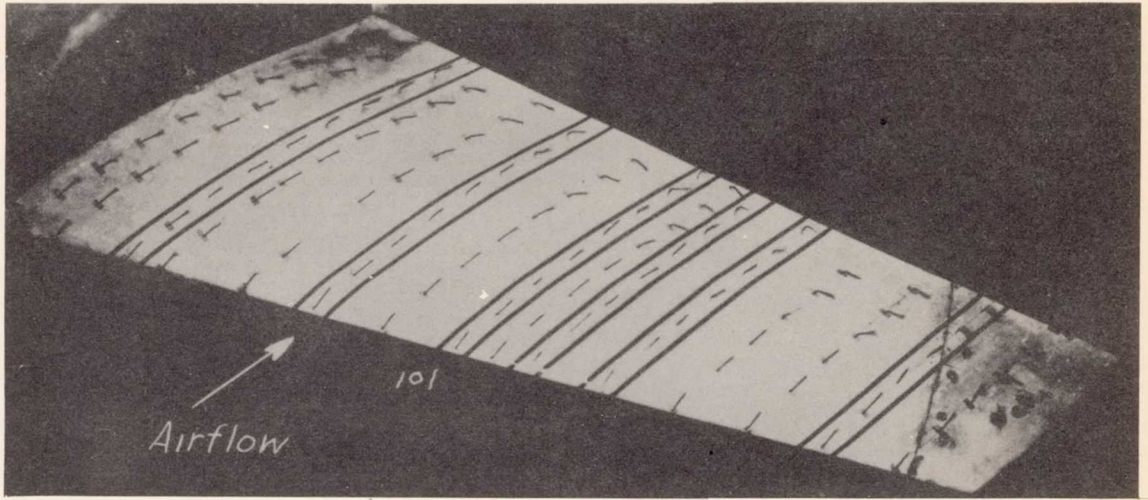
$$\alpha = 16^{\circ}$$



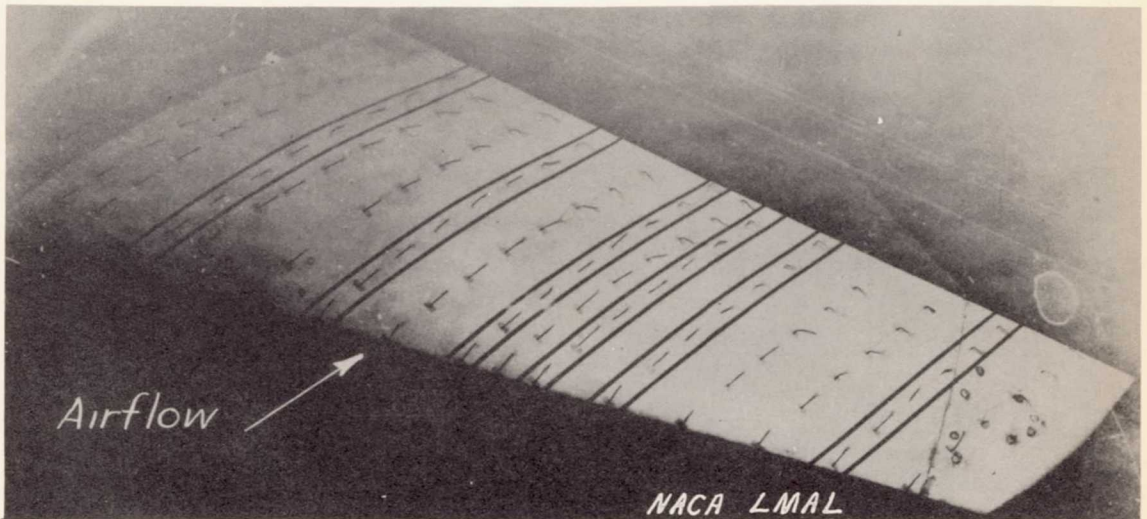
$$\alpha = 17^{\circ}$$

(c) $\alpha = 16^{\circ}, 17^{\circ}$.

Figure 11.- Continued.



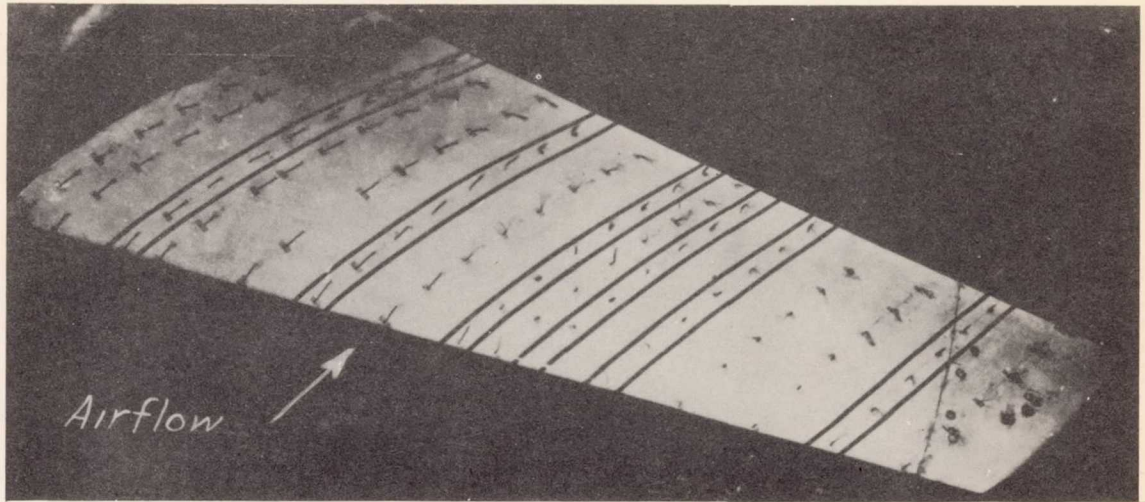
$$\alpha = 18^\circ$$



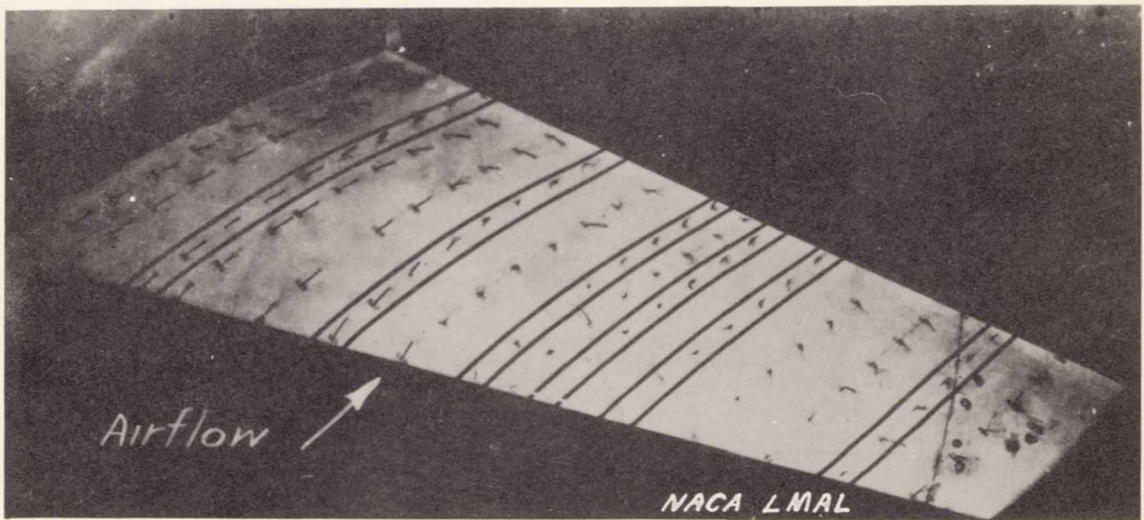
$$\alpha = 19^\circ$$

(d) $\alpha = 18^\circ, 19^\circ$.

Figure 11.- Continued.



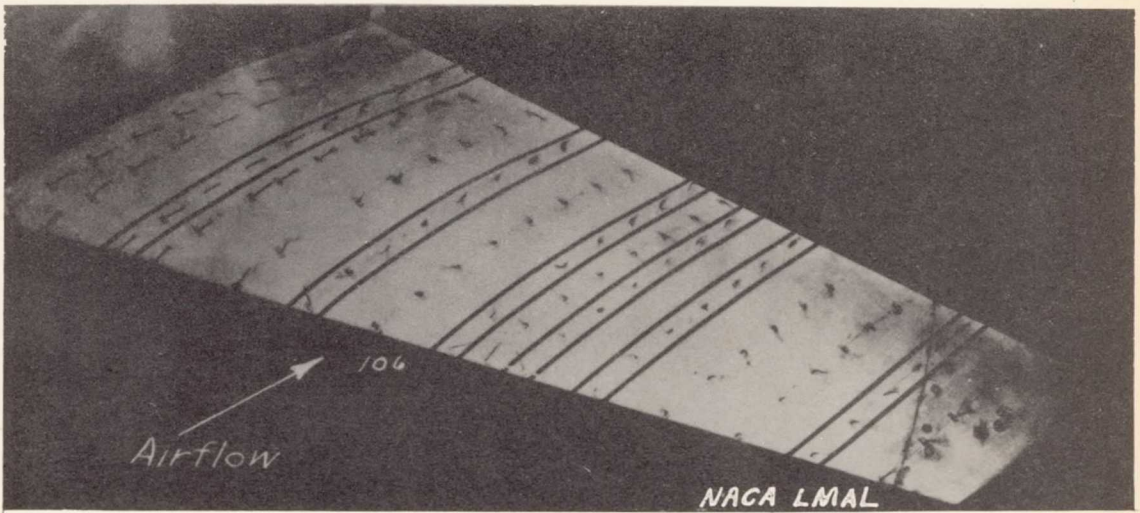
$\alpha = 20^\circ$



$\alpha = 21^\circ$

(e) $\alpha = 20^\circ, 21^\circ$.

Figure 11.- Continued.



(f) $\alpha = 22^\circ$.

Figure 11.- Concluded.

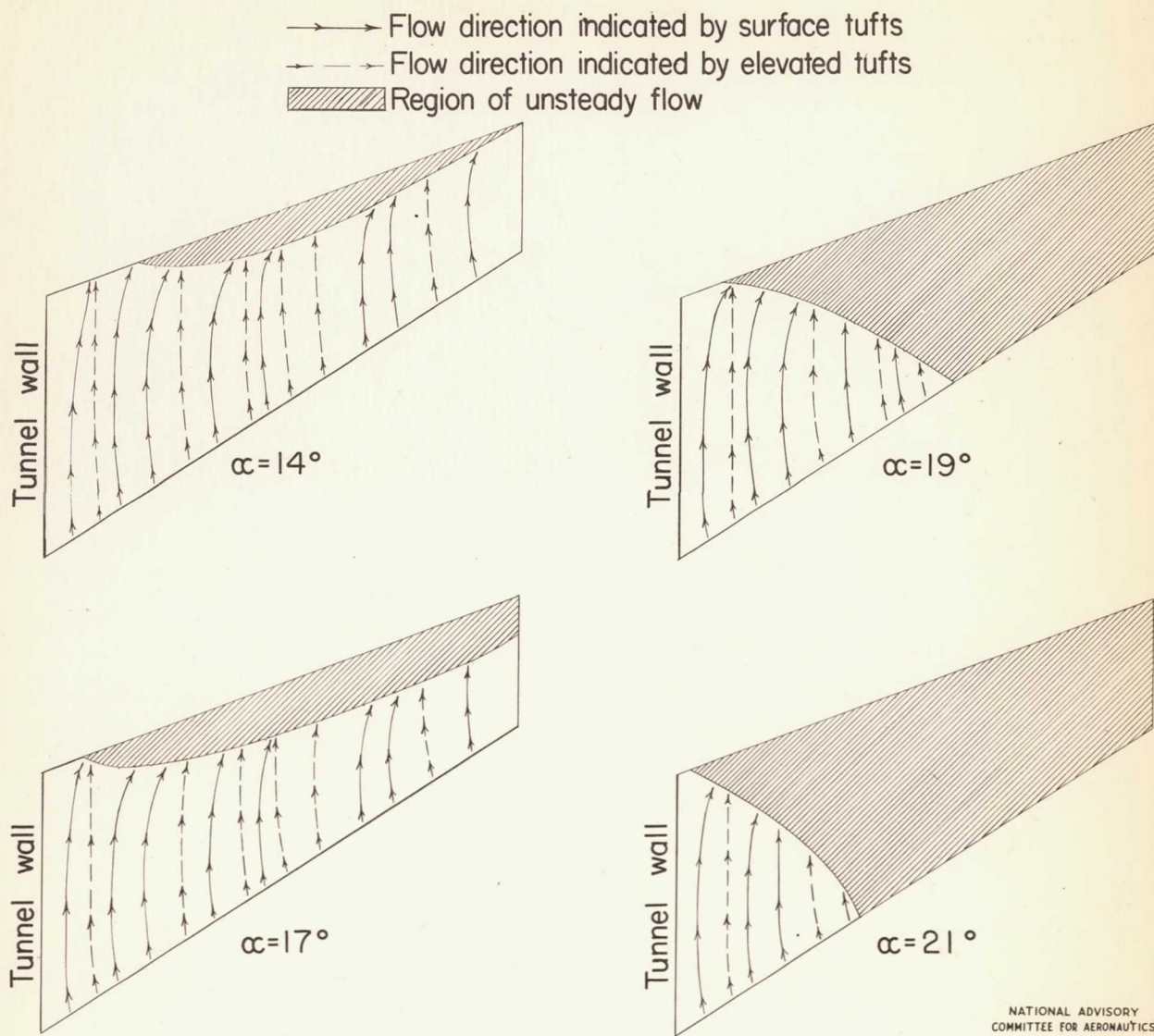
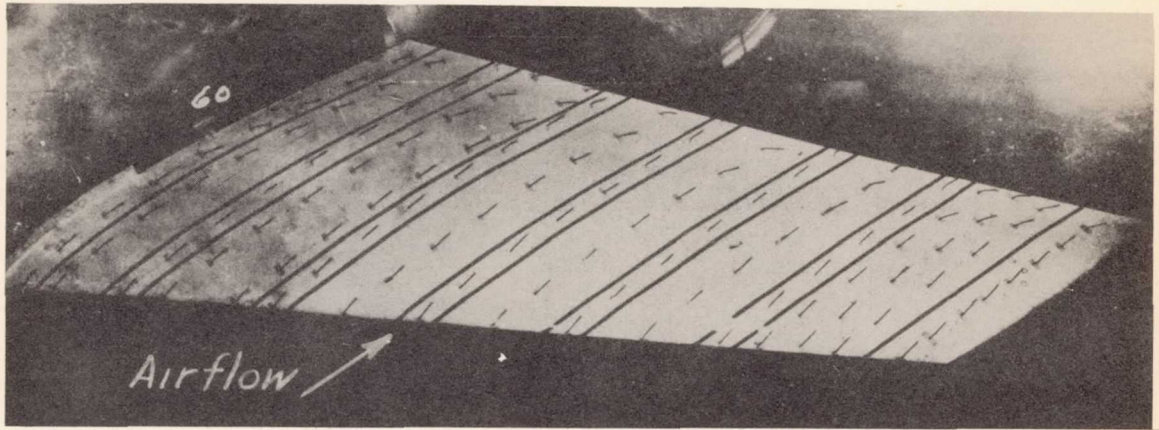
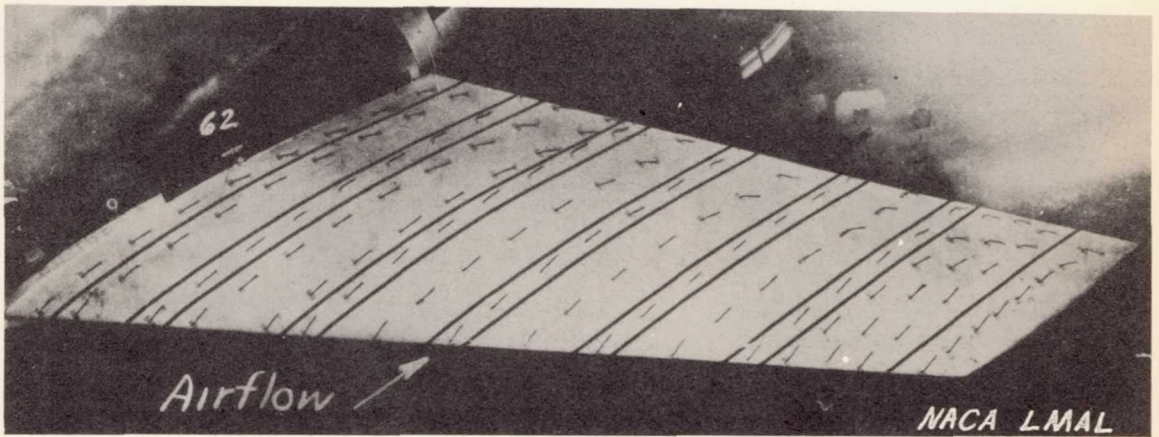


Figure 12.—Flow patterns indicated by tufts on a 65₂-215 wing at various angles of attack. $\Lambda = 30^\circ$. $M = .13$.



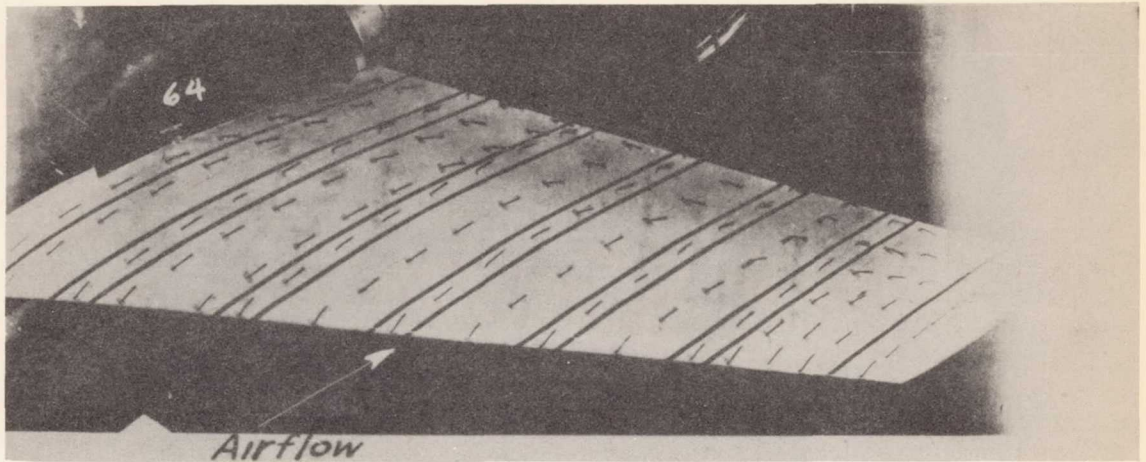
$$\alpha = 8^{\circ}$$



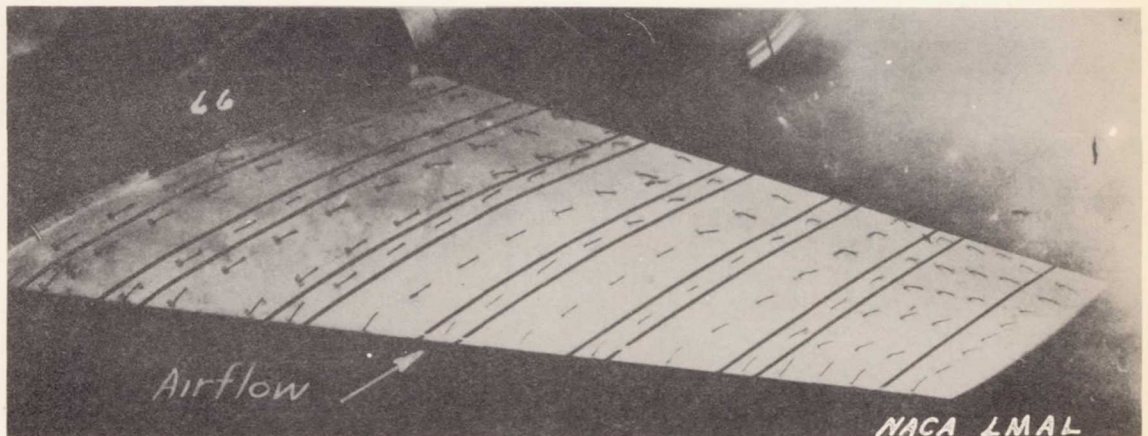
$$\alpha = 12^{\circ}$$

(a) $\alpha = 8^{\circ}, 12^{\circ}$.

Figure 13.- Tuft patterns on a 65_2 -215 wing, $\Lambda = 45^{\circ}$, $M = 0.13$.



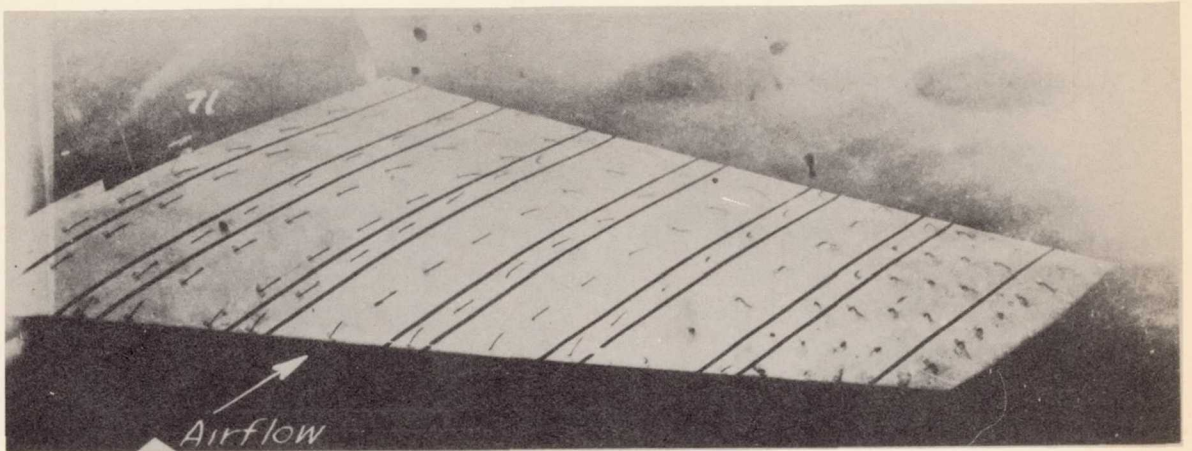
$\alpha = 16^\circ$



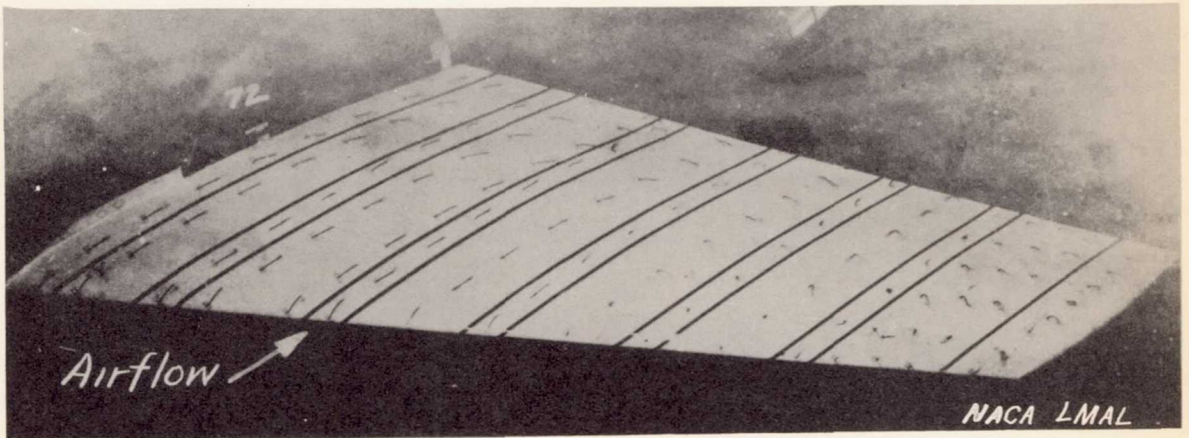
$\alpha = 18^\circ$

(b) $\alpha = 16^\circ, 18^\circ$.

Figure 13.- Continued.



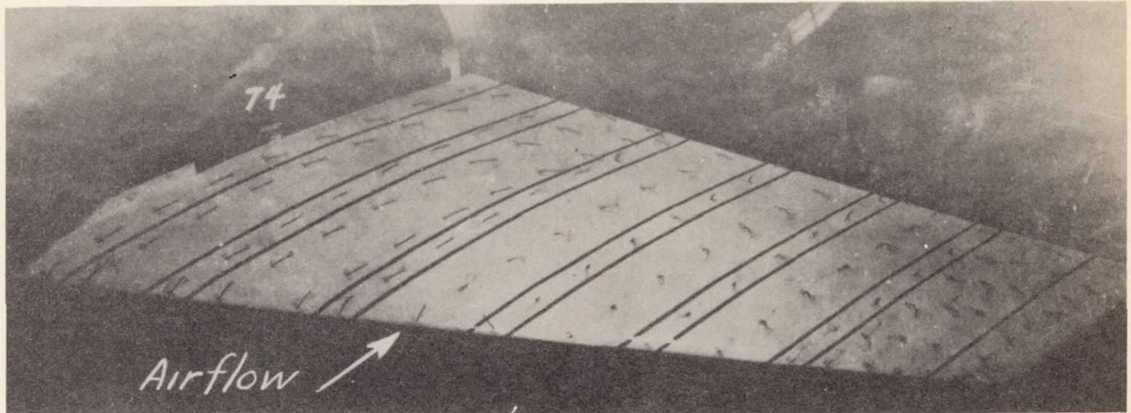
$$\alpha = 19^\circ$$



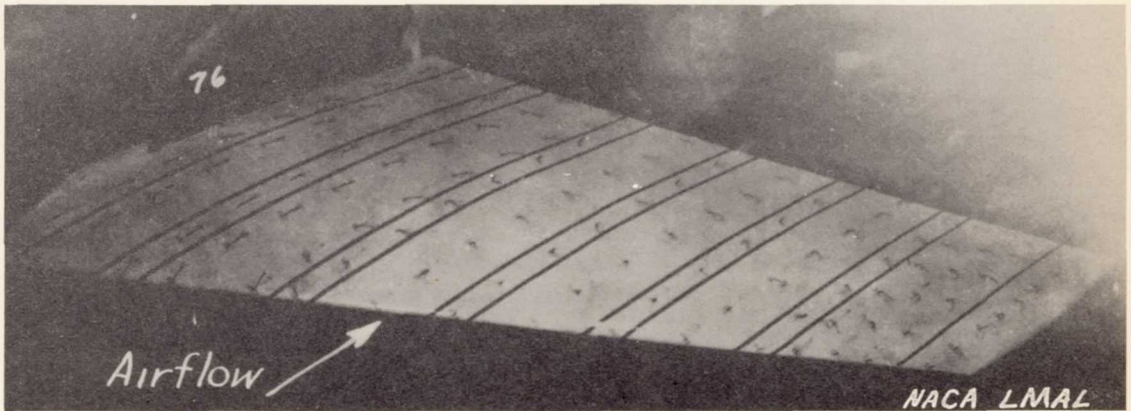
$$\alpha = 20^\circ$$

(c) $\alpha = 19^\circ, 20^\circ$.

Figure 13.- Continued.



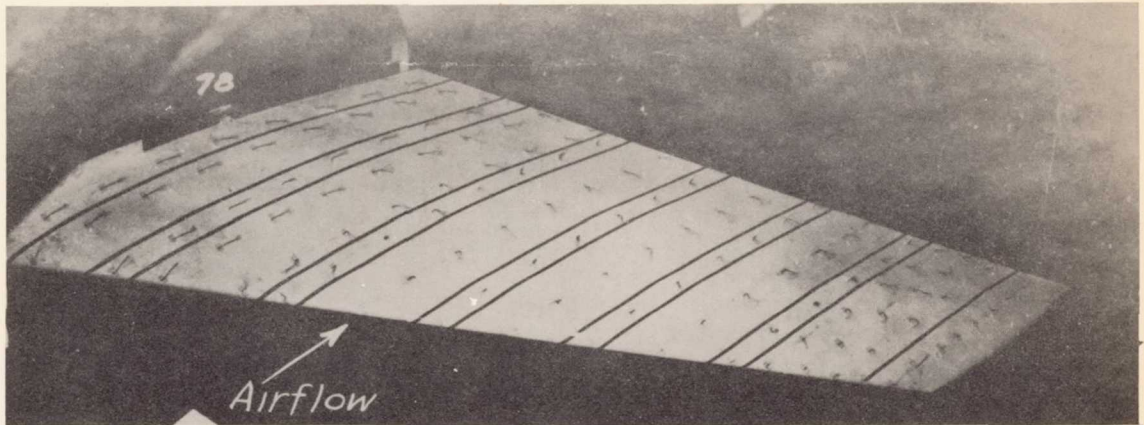
$$\alpha = 22^\circ$$



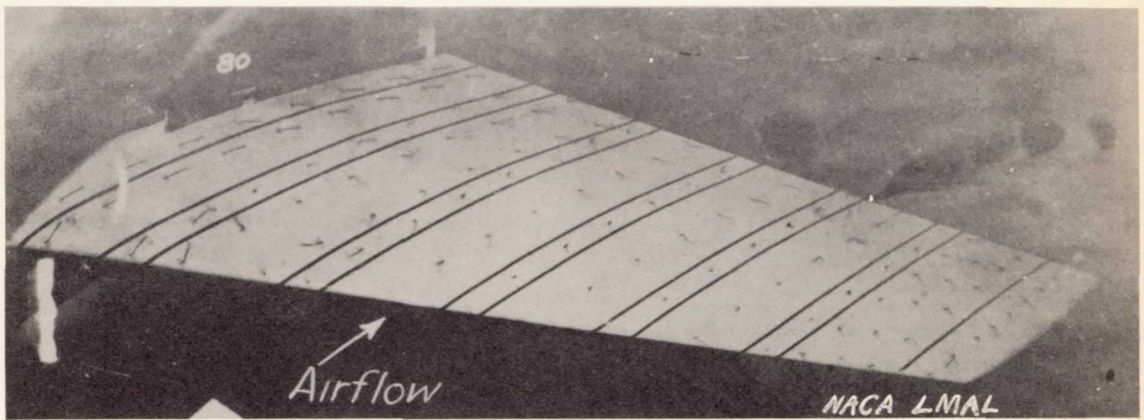
$$\alpha = 24^\circ$$

(d) $\alpha = 22^\circ, 24^\circ$.

Figure 13.- Continued.



$$\alpha = 26^{\circ}$$

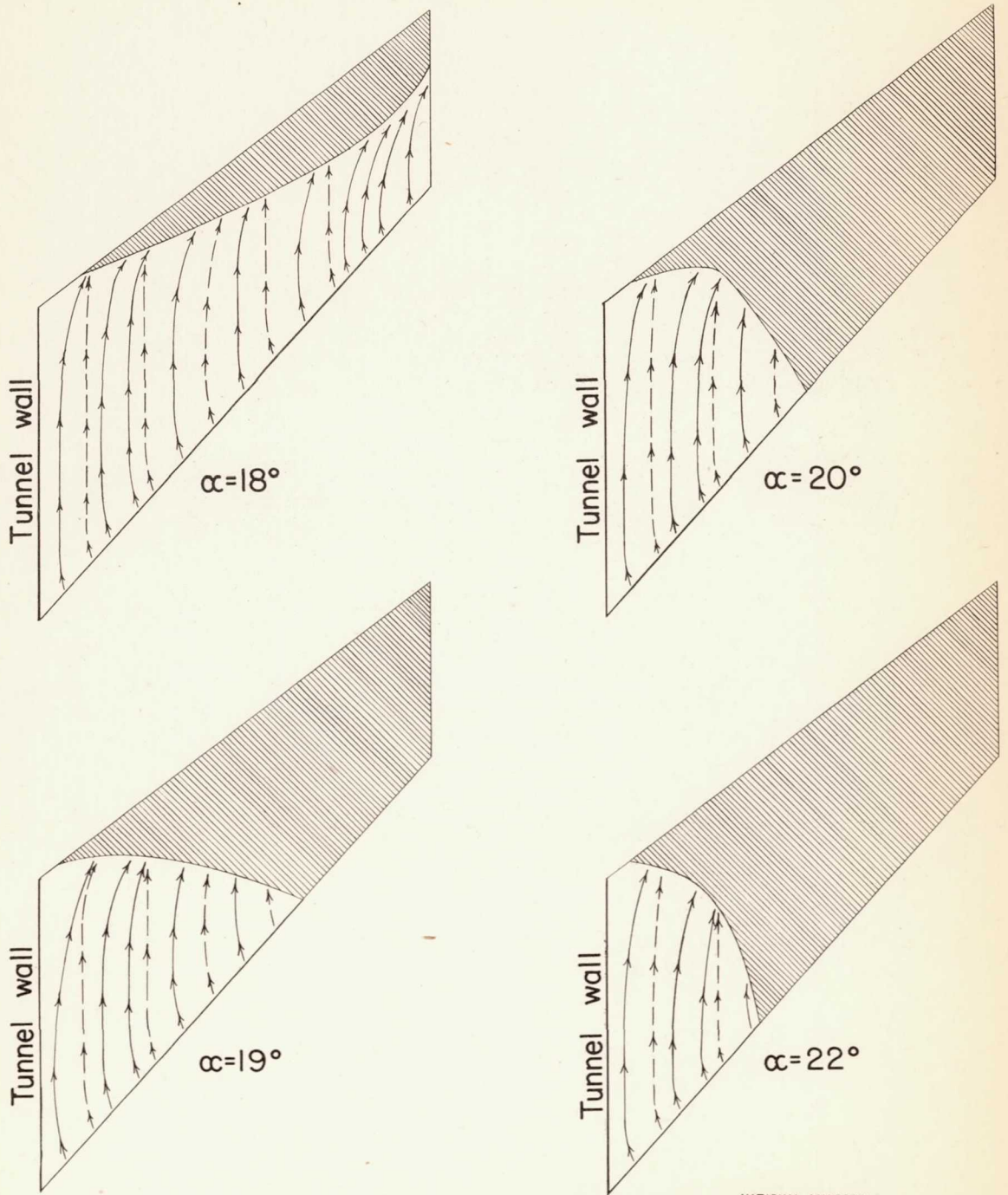


$$\alpha = 28^{\circ}$$

(e) $\alpha = 26^{\circ}, 28^{\circ}$.

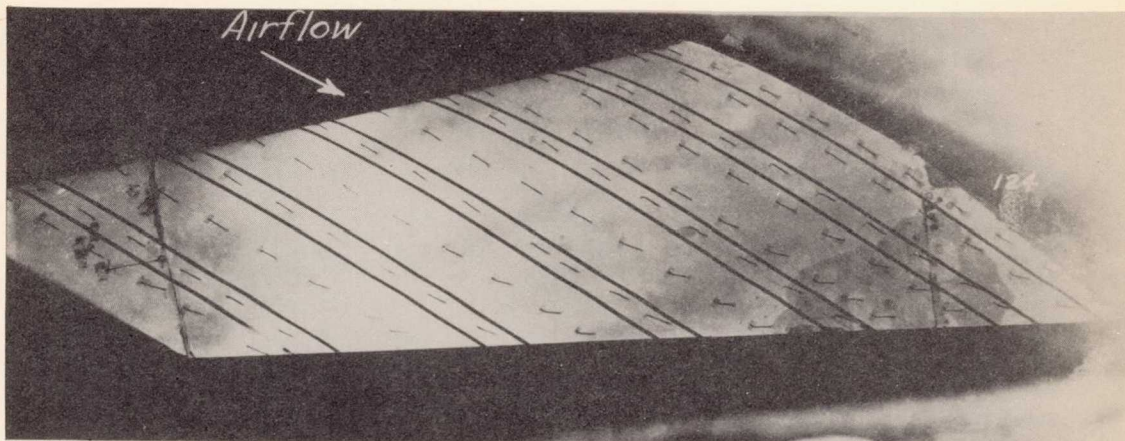
Figure 13.- Concluded.

- Flow direction indicated by surface tufts
- - - - - Flow direction indicated by elevated tufts
- ▨ Region of unsteady flow

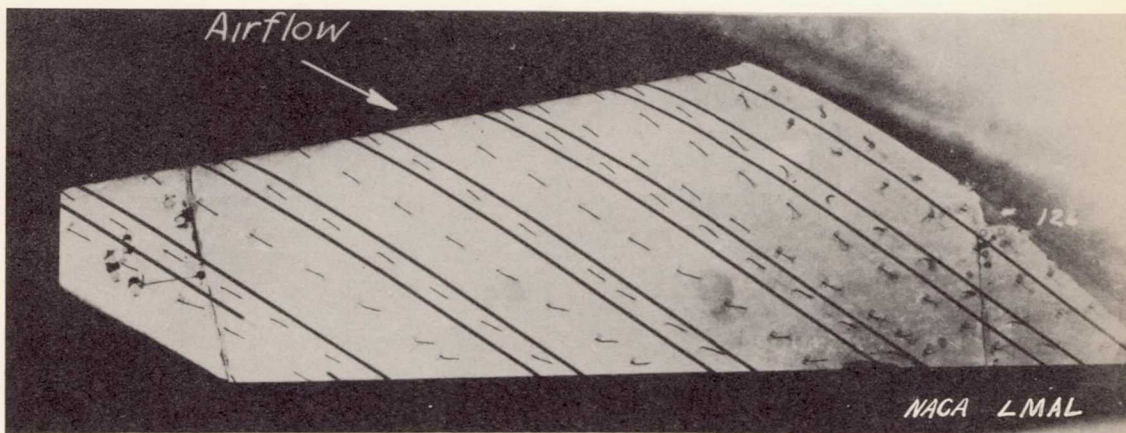


NATIONAL ADVISORY
COMMITTEE FOR AERONAUTICS

Figure 14.—Flow patterns indicated by tufts on a 65₂-215 wing at various angles of attack. $\Lambda = 45^\circ$. $M = .13$.



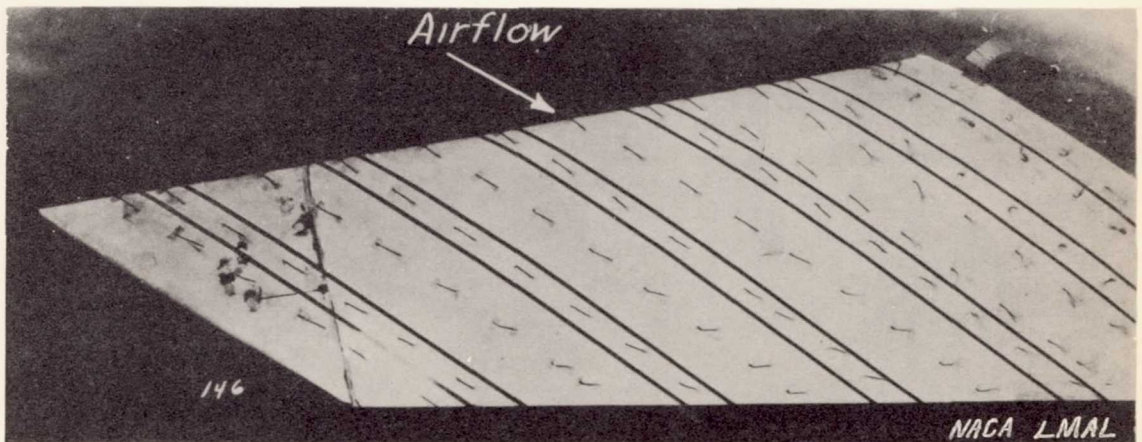
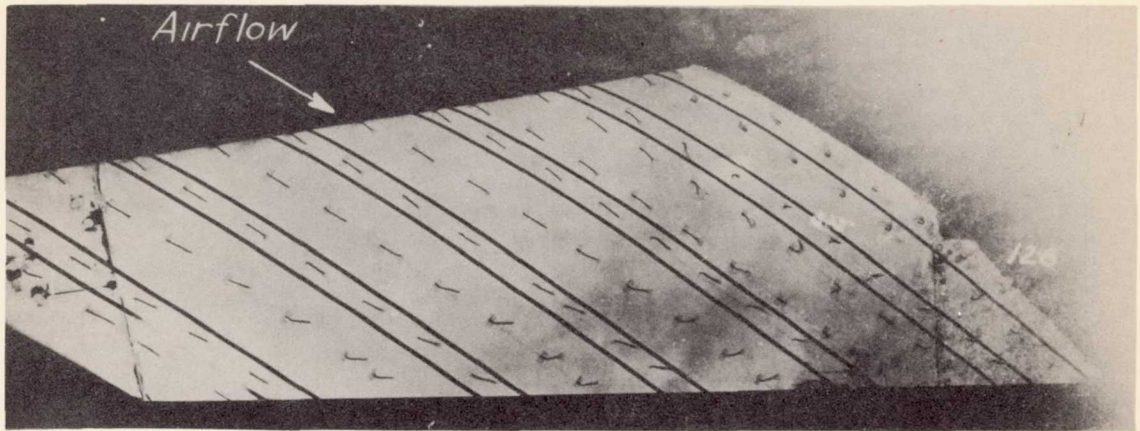
$$\alpha = 8^\circ$$



$$\alpha = 12^\circ$$

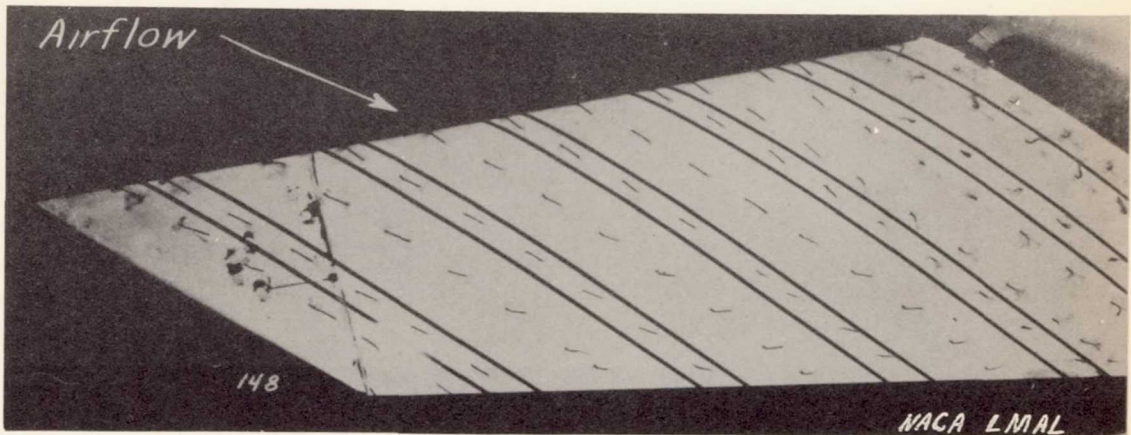
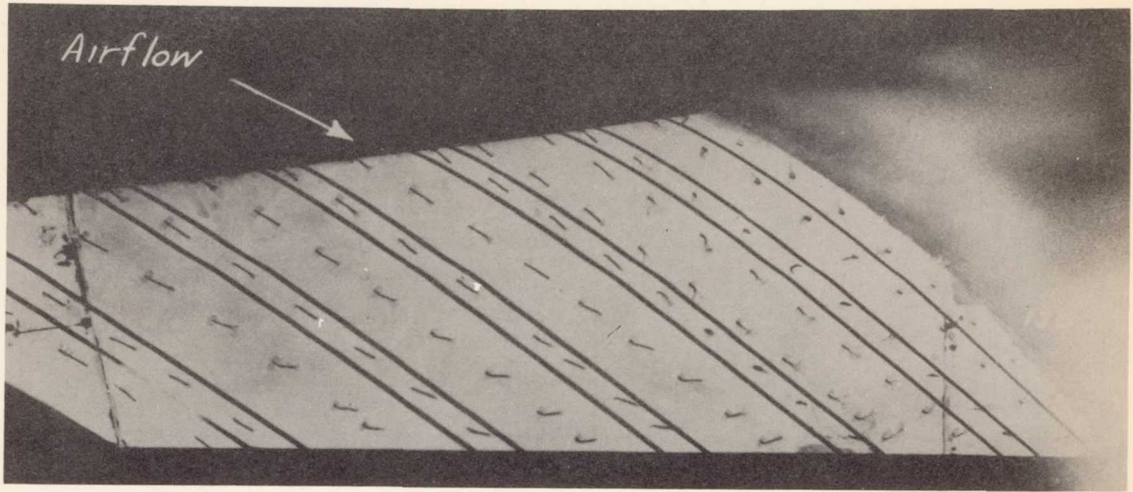
(a) $\alpha = 8^\circ, 12^\circ$.

Figure 15.- Tuft patterns on a 65₂-215 wing, $\Lambda = -45^\circ$, $M = 0.13$.



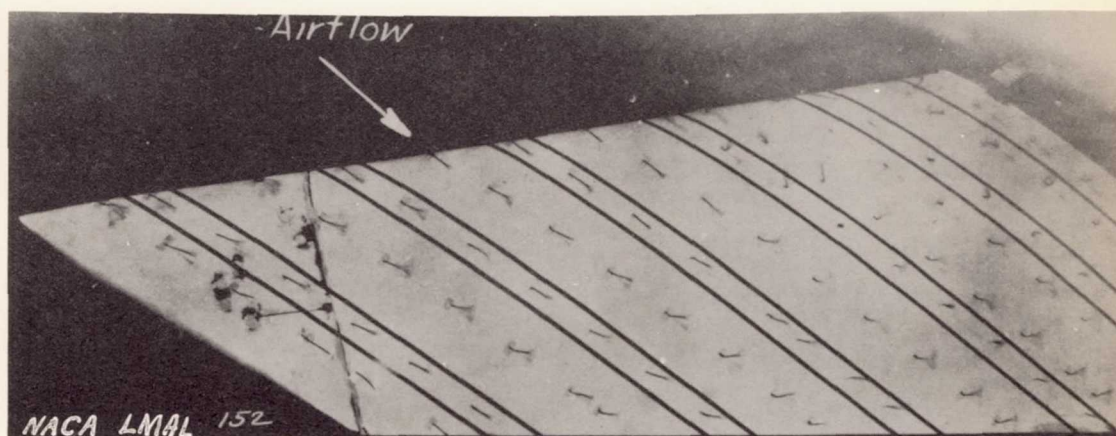
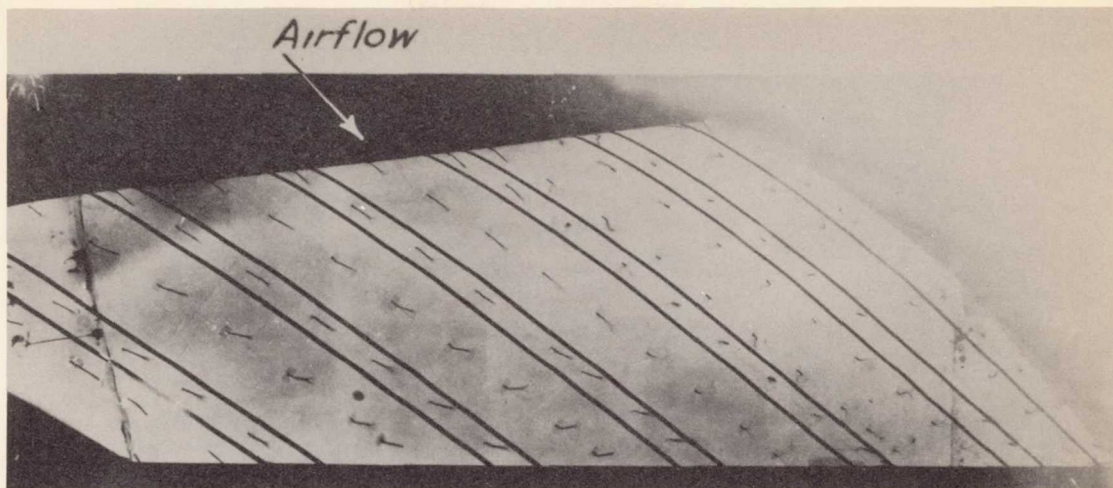
(b) $\alpha = 16^\circ$.

Figure 15.- Continued.



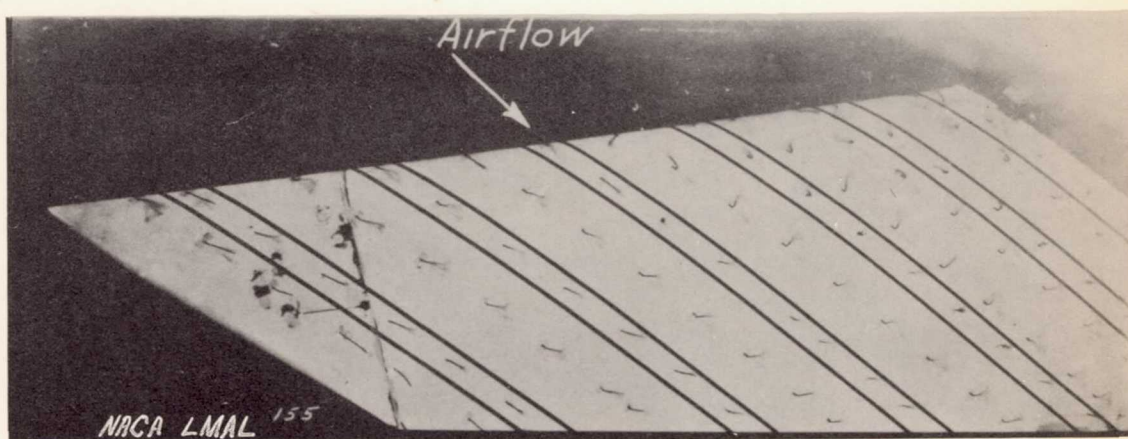
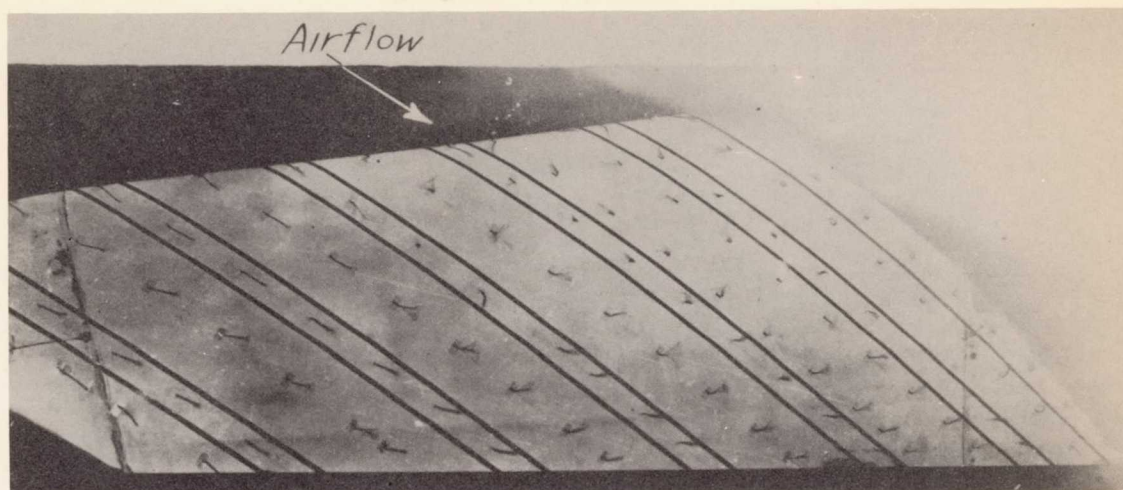
(c) $\alpha = 18^\circ$.

Figure 15.- Continued.



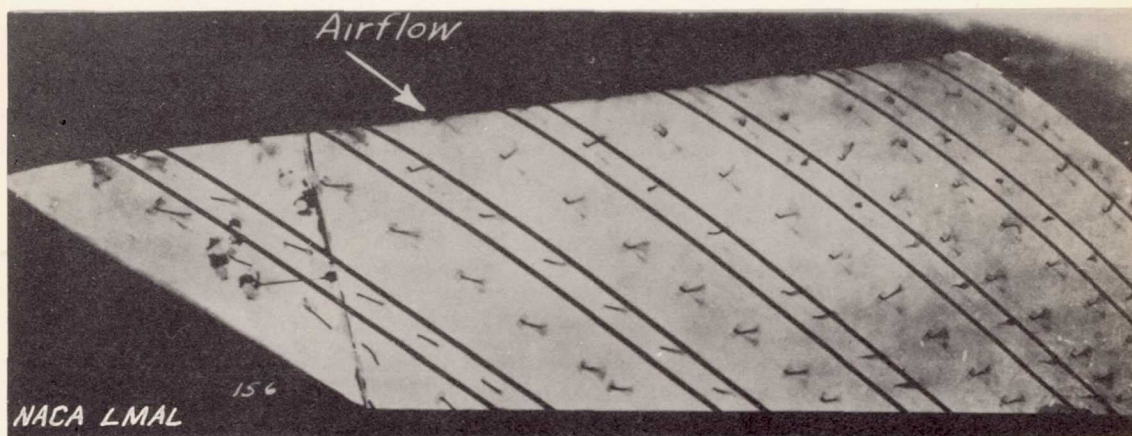
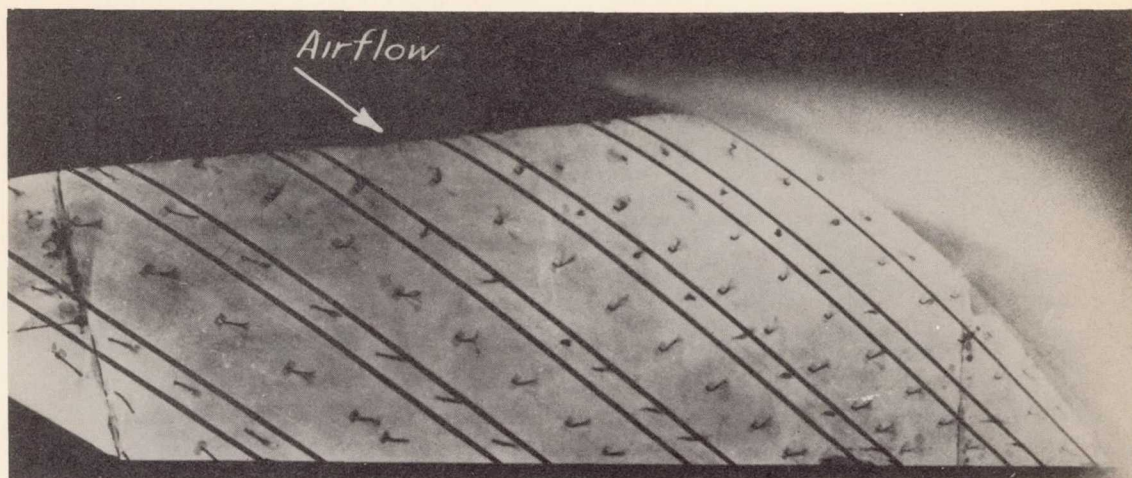
(d) $\alpha = 20^\circ$.

Figure 15.- Continued.



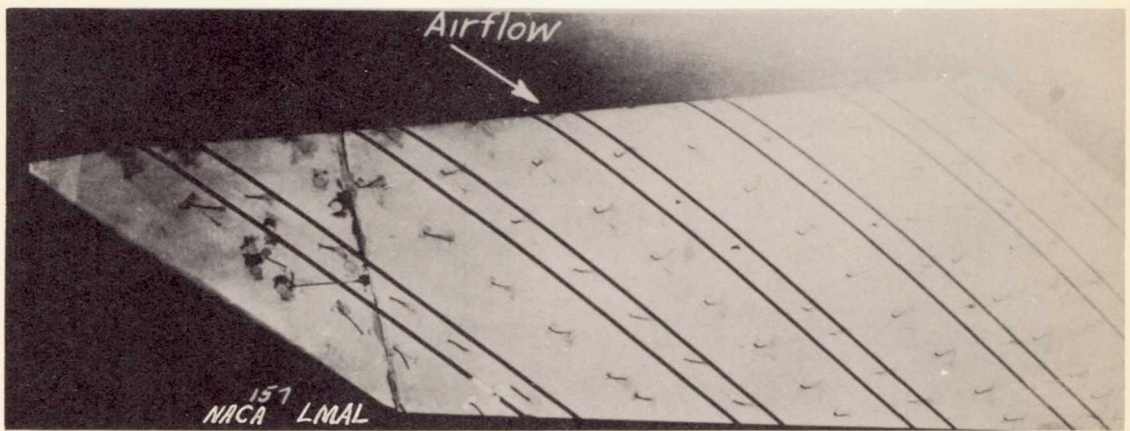
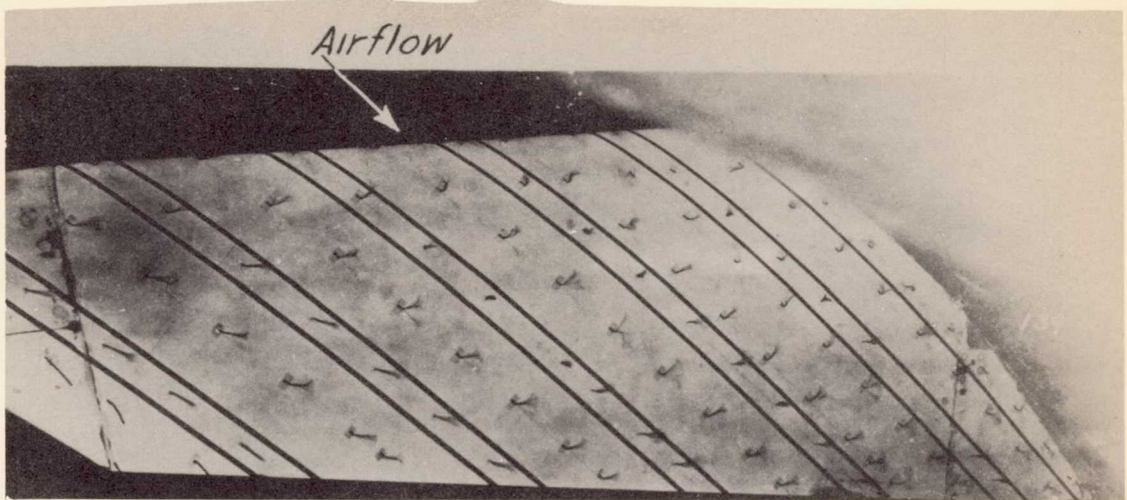
(e) $\alpha = 22^\circ$.

Figure 15.- Continued.



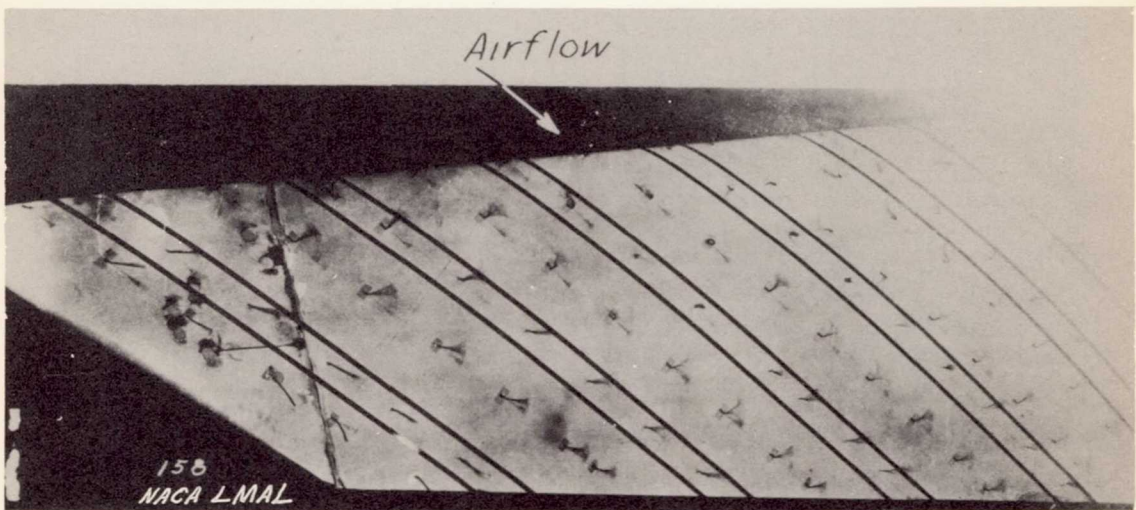
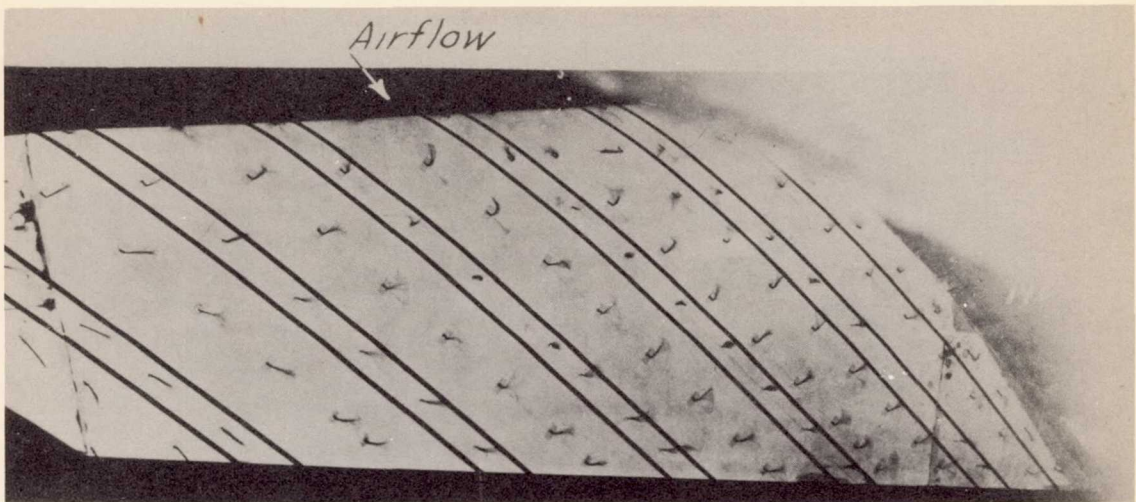
(f) $\alpha = 24^{\circ}$.

Figure 15.- Continued.



(g) $\alpha = 26^{\circ}$.

Figure 15.- Continued.



(h) $\alpha = 28^\circ$.

Figure 15.- Concluded.

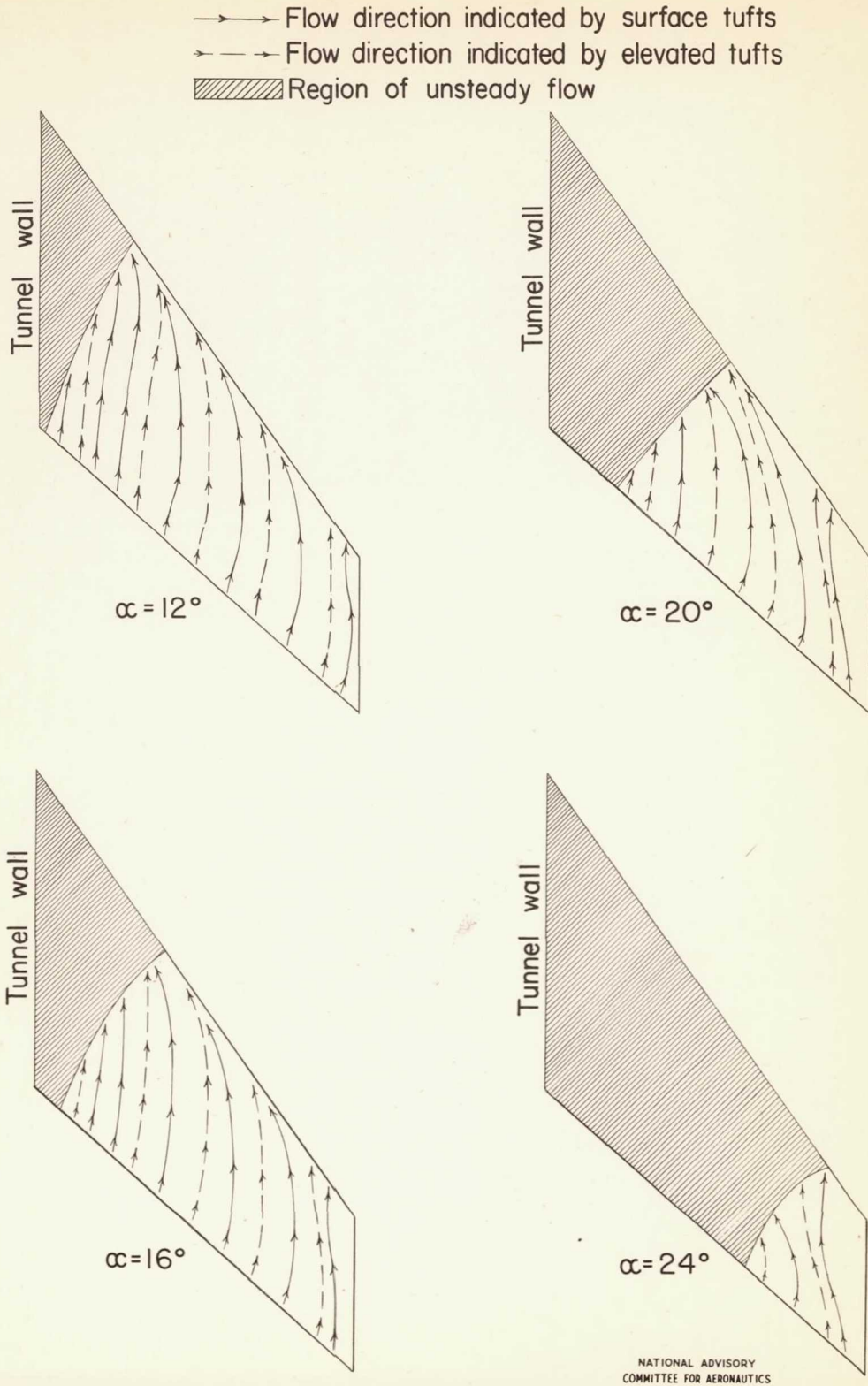


Figure 16.— Flow patterns indicated by tufts on a 65₂-215 wing at various angles of attack. $\Lambda = -45^\circ$. $M = .13$.